



FCTUC FACULDADE DE CIÊNCIAS
E TECNOLOGIA
UNIVERSIDADE DE COIMBRA

DEPARTMENT OF MECHANICAL
ENGINEERING

Switchable magnets for robotics applications

Dissertation presented to achieve the degree of Master in Mechanical Engineering in the specialization of Energy and Environment

Author

José Carlos Romão

Supervisors

Prof. Dr. Mahmoud Tavakoli

Prof. Dr. Pedro Neto

Jury

President Professor Doctor **Cristóvão Silva**
Auxiliar Professor from University of Coimbra

Members Engineer **Carlos Viegas**
Ph. D. researcher from Institute of Systems and Robotics
Professor Doctor **Mahmoud Tavakoli**
Post-doc researcher from Institute of Systems and Robotics

Institucional coloboration



Coimbra, September, 2014

Sempre chegamos ao sítio aonde nos esperam.

José Saramago

À minha mãe.

ACKNOWLEDGEMENTS

This work would not have been possible without the people who with their wisdom and fellowship spent time and energy following my work and helping me when I needed.

Thanks to Professor Pedro Neto, who since the beginning of this research work helped calm me down when I was worried or didn't feel capable to overcome the challenges that this dissertation imposed and would rather work with me on an uncomplicated approach to the arising difficulties.

Thanks to Professor Mahmoud Tavakoli. His strategy of letting that the discussion of the problems and opportunities that raised at every step we gave set up the next task to do had a major role on my motivation on doing this work.

Thanks to Carlos Viegas, who had a major role on introducing me to the work developed on ISR. Since the beginning of my work he closely followed my steps and was responsible for many of the ideas I implemented in the robot's design.

Thanks to Rafael Batista, who was my thesis colleague during this semester. He closely followed my work with interest and shared with me his knowledge about the topics we were working on.

Thanks to Pedro Lopes, who helped me with the control of the actuators and with other code and electronic issues.

Thanks to David Santos for helping me to understand how the novel climbing robot should be designed.

Finally, thanks to the friends I made during my academic course here in Coimbra: Alexandre, Artur, Diogo, Jorge, Leandro, Marcelo, Miguel, Pedro, amongst many others... Without your friendship this time of my life would have been so much more boring...

ABSTRACT

The goal of this work is to produce an optimized switchable magnet to be used in small robotic applications. A switchable magnet is a system which uses moving permanent magnets to change the magnetic flux path and switch on or off the magnetic attraction force.

The most relevant magnetic holders are presented and their working principle is explained. Then, a switchable magnet model is introduced on the *Comsol Multiphysics*, a physics simulation software, to enable a better understanding of its working principles, and the effect of different design and material parameters on the attraction force of the unit. Still in *Comsol* more simulations are exposed with the goal of making a similar device in a smaller scale with the best holding force per unit mass, whose magnetic fields interact in a constructive or destructive way, changing the path of the magnetic flux. We then coupled this device with an actuator in order to control its state (on/off).

Then, two robotic devices using the novel switchable magnet are designed. The first one is a holding mechanism for a climbing robot, whose design relies on electromagnets. The second one is a prototype of a climbing robot which moves like a scissor, taking advantage of two ends which contain switchable magnets. In both systems the application of switchable magnets has one clear advantage, that is, in contrary to electromagnets this device only consumes energy at the time of switching the force on and off. The purpose of these two applications is to demonstrate the potential of the switchable magnets and show their great advantage (only requiring power to switch between states): magnetic force control without constant power feed.

Keywords Climbing robots, Magnetic holders, Switchable magnets.

CONTENTS

1.	Introduction.....	1
1.1.	Structure.....	1
1.2.	Motivation.....	2
2.	Magnetic holding devices.....	5
2.1.	Introduction.....	5
2.2.	Permanent magnets.....	5
2.2.1.	Physical background.....	5
2.2.2.	Magnetic force.....	8
2.2.3.	Types.....	9
2.3.	Electromagnets.....	10
2.3.1.	Physical background.....	10
2.4.	Electropermanent magnets.....	12
2.4.1.	Types.....	13
2.5.	Switchable magnets.....	14
2.5.1.	Types.....	14
2.5.2.	Applications in robotics.....	17
2.5.3.	<i>MagJig 95</i>	19
3.	Simulation.....	21
3.1.	Introduction.....	21
3.2.	<i>Comsol</i> Multiphysics.....	21
3.3.	Materials defined in <i>Comsol</i>	22
3.3.1.	Magnets.....	22
3.3.2.	Housing.....	23
3.3.3.	Anti-friction disc.....	24
3.3.4.	Leakage stopper disc.....	25
3.3.5.	Attachment plate.....	25
3.4.	Simulations.....	25
3.4.1.	Simulation of the commercial device.....	26
3.4.2.	Modifications.....	27
4.	A new optimized switchable magnet.....	33
4.1.	Introduction.....	33
4.2.	Magnets.....	35
4.3.	Housing.....	35
5.	OmniClimber magnetic holding device.....	45
5.1.	Introduction.....	45
5.2.	Design.....	45
5.3.	Features.....	46
5.4.	Testing.....	47
6.	Climbing robot.....	49
6.1.	Introduction.....	49

6.2.	Operation	49
6.3.	Design.....	51
6.4.	Features.....	55
7.	Conclusion.....	57
7.1.	Possible developments.....	58
7.1.1.	<i>OmniClimber</i> magnetic holding device.....	58
7.1.2.	Climbing robot.....	58
7.1.3.	Electropermanent magnet.....	59
8.	List of references	61
9.	Appendix.....	63

INDEX OF FIGURES

Figure 1.1 The REST, a climbing robot intended for welding in ferromagnetic walls. ^[2]	2
Figure 1.1 Comparison between the effect of the distance to the surface between permanent magnets and electromagnets.	3
Figure 2.1 Magnetic hysteresis, in which B is the magnetization of the material, H the magnetic field, m_{rs} the remanence and h_c the coercivity.	6
Figure 2.2 Maximum energy product of a magnet. ^[5]	7
Figure 2.3 Effects of Curie temperature: a) Below the Curie temperature, neighbouring magnetic spins align ^[7] , b) Above the Curie temperature, the magnetic spins are randomly aligned ^[8]	8
Figure 2.4 Magnet at a distance s from the surface.	8
Figure 2.5 Effects of Ampere's circuital law: a) magnetic field created around a wire ^[10] , b) created around a loop ^[11]	11
Figure 2.6 Magnetic field created around a solenoid. ^[12]	11
Figure 2.7 Operation of a magnetic plane: a) off state: the low coercive magnets 8 were magnetized in the same direction as the high coercive magnets 6 by the passage of an electrical pulse through the coils 10 in a suitable sense, b) on: the magnets 8 have their magnetic fields established opposite to that of magnets 6 by the pulsed energization of coils 10 in the opposite sense. ^[15]	13
Figure 2.8 Operation of a parallel electro permanent magnet. ^[16]	14
Figure 2.9 Neptune magnetic holder: a) configuration, b) off state, c) on. ^[21]	15
Figure 2.10 Variable magnet: a) configuration, b) off state: when the device is off, the north magnetic area of the surface of core is coincident with the south magnetic area of the inner surface of the sleeve 11, c) on: as the core 10 is rotated with respect to the sleeve 11, the flux travels between the opposite poles that are getting apart between each other's and the magnetic fields are increasing until, at 180 degrees, the magnet is on. ^[18]	15
Figure 2.11 operation of a magnetic plane: a) off: with both magnets facing opposite directions aligned, the device is off, b) on: rotating the crank aligns the magnets, making the magnetic flux circulate outside the device only. ^[19]	16
Figure 2.12 Operation of a H-type device: a) off: all the flux goes between the poles through both u-shaped iron parts, b) on: by turning the magnet by 90° degrees, the flux goes from North Pole through one u-shaped iron, through the plate and the second u-shaped iron to the South Pole. ^[17]	16
Figure 2.13 Configuration of a H-type double magnets device ^[20]	17
Figure 2.14 Operation of a H-type double magnets device: a) off: the upper magnet 11 is positioned such that its north pole substantially overlies the south pole of first	

magnet 10, so the magnetic flux travels from one magnet to another inside the device, b) on rotating the upper magnet 11 180° about its axis of rotation brings the magnets into the alignment and the magnetic flux follows a path outside of the device.	17
Figure 2.15 Crawler of the <i>Neptune</i> ^[21]	18
Figure 2.16 <i>Miche</i> robot: a) initial configuration, b) possible alignment. ^[22]	18
Figure 2.17 Model range of the <i>MagJig</i> models from <i>Magswitch</i> (the model number relates to the holding force in pounds). ^[23]	19
Figure 2.18 Holding force and holding force per unit mass	20
Figure 3.1 Section of the <i>MagJig 95</i> : 1) magnets, 2) housing, 3) anti-friction disc, 4) leakage stopper disc.	22
Figure 3.2 Magnet description. ^[6]	23
Figure 3.3 <i>MagJig 95</i> model made in a CAD software with dimensions in millimeters. ...	23
Figure 3.4 Hysteresis curve of the housing material, provided by <i>Magswitch</i>	24
Figure 3.5 Section of the housing.	26
Figure 3.6 Section of the simulated device: 1) magnets, 2) housing, 3) anti-friction disc.	27
Figure 3.7 Circular housing made in a CAD software with dimensions in millimeters.	28
Figure 3.8 Plastic housing: a) CAD model, b) assembled.	30
Figure 4.1 <i>OmniClimber VI</i> transition mechanism. ^[26]	33
Figure 4.2 <i>OmniClimber</i> support with electromagnets. ^[26]	33
Figure 4.3 Electromagnet advertised force. ^[3]	34
Figure 4.4 Torque resulting from different shapes of the device:	34
Figure 4.5 Magnet description. ^[6]	35
Figure 4.6 Absolute force and force per unit mass.	37
Figure 4.7 Experimental testing	37
Figure 4.8 Comparison between the magnetic field of the <i>MagJig 95</i> and of the novel device: a) 7 mm thick plate, b) 1 mm thick plate.	39
Figure 4.9 Difference between the <i>Comsol</i> results and the experiments.	43
Figure 4.10 adjustment of a polynomial to <i>Comsol</i> value	43
Figure 5.1 Operation of the device: a) initial position, b) the <i>OmniClimber</i> is raised, c) It reaches the surface, d) the permanent magnets makes it attach to the surface.	45
Figure 5.2 Degrees of freedom accomplished by the transmission axle of the switchable magnets.	46
Figure 5.3 <i>OmniClimber</i> support with switchable magnets on a curved surface.	46
Figure 5.4 Transmission mechanism, with actuator (1) and transmission mechanism (2).	47
Figure 5.5 Experiment on a curved surface: a) switchable magnets off, b) on.	48

Figure 5.6 Plane transition: initial position, with the center of the <i>OmniClimber</i> 13.5 cm away from the wall, b) the robot is raised, c) the <i>OmniClimber</i> is fixed to the wall by a permanent magnet, d) It is lowered down by the arm, e) It is again on initial position.	48
Figure 6.1 <i>SkySweeper</i> . ^[29]	49
Figure 6.2 Robot behavior - the on (fixed) magnet is at red and the off (loose) at green: a) the upper magnet is off and the lower is on, and the robot is fully closed, b) the motor drives the links in order to depart from each other, c) the robot reaches its maximum extension, d) the motor turns on the opposite direction and the links begin approaching each other, e) the robot is again fully closed.	50
Figure 6.3 Configuration: a) motor that drives the links, b) pulley, c) motor that actuates the magnet, d) switchable magnet, e) bearing, f) permanent magnet.....	50
Figure 6.4 Free body diagram: a) forces from which the torque on the axis 1 depends, b) forces from which the torque on the axis 2 depends.	51
Figure 6.5 First prototype (with longer links).	54
Figure 6.6 Operation (see Figure 6.2).	54
Figure 6.7 Base, with AX-12 (1), <i>Robotis</i> kit part (2), axle holder (3), magnetic support (4), switchable magnet (5), bearings (6) and permanent magnets (7).	55
Figure 6.8 Climbing robot, with bases (1), transverse bars (2) and MX-64 (3).	56
Figure 7.1 On a small section pipe.	58
Figure 7.2 Base with springs.	59
Figure 7.3 <i>Project Ara</i> cellphone ^[31]	59

INDEX OF TABLES

Table 2.1. Comparison between each type.....	10
Table 2.2. Comparison between each model.....	19
Table 3.1. Composition of the housing metal ^[22]	24
Table 3.2. Base model.....	26
Table 3.3. Base model on a plate 1 mm thick	27
Table 3.4. Without air gap.....	28
Table 3.5. Circular housing	29
Table 3.6. Plastic housing	29
Table 3.7. Comparison between simulation and practical experiment	30
Table 3.8. Diameter of 28 mm.....	31
Table 3.9. Diameter of 26 mm.....	31
Table 3.10. Comparison between the simulations	32
Table 4.1. Comparison between each design	36
Table 4.2. Novel device on a plate 1 mm thick	38
Table 4.3. Comparison between the <i>MagJig 95</i> and the novel device	38
Table 4.4. Comparison between the electromagnet and the novel device	40
Table 4.4. Comparison between the electromagnet and the novel device with an actuator	40
Table 4.5. Holding force depending on the angle.....	42
Table 6.1. Constant values	53
Table 6.2. Updated constant values	54

1. INTRODUCTION

1.1. Structure

This dissertation is composed of seven chapters.

On this first chapter we make an introduction to the subject of magnetic devices applied to climbing robots, focusing on the different technologies employed, like electro and switchable magnets. Then we discuss the goals set for this research work and explain the motivation behind it.

On Chapter 2 we analyze the four different types of magnetic technologies: permanent magnets, electromagnets, electropermanent magnets and switchable magnets. The physical basis needed for the comprehension of each concept is provided. Then we explain the operation of some of the more relevant models, whereas because they are the most common solutions employed in this field or because of their value in the evolution of the concept. Finally we make a quick view of the *MagJig 95* device, and the rest of the model range, which we propose to study and adapt to a novel application in climbing robots.

On Chapter 3 we use *Comsol Multiphysics* to better understand the role of the different *MagJig 95* design aspects and their effect on the magnetic attraction force provided by the device. The objective here is to see if the device can be improved in terms of force to weight ratio or if it is already an optimized solution.

On Chapter 4 we set out to design a smaller device based on the *MagJig 95*, to be used on small robotic applications, bearing in mind the conclusions we drew from the *Comsol* tests made on the previous chapter and new simulations made to evaluate extra parameters. The novel design developed is thoroughly simulated and a prototype is assembled and tested to validate these simulations.

On Chapter 5 we design a novel support for *OmniClimber* with switchable magnets. Its working principle and most important features are explained and experimental tests with a working prototype are made and discussed.

On Chapter 6 a novel climbing robot employing switchable magnets as main adhesion mechanism is designed. Both concept and detail design are presented, as well as the experimental test conducted with a fully functional prototype.

Finally on the last chapter, we discuss this work's achievements and possible future developments.

1.2. Motivation

Climbing robots are devices which are useful in a variety of applications, specially for maintenance and inspection of elevated structures, such as reservoirs, bridges, pipes, etc. This kind of operations usually involves a high number of unsafe manual operations and represents a danger even for skilled workers. This explains the growing interest in the development of climbing robots in the last years. The development of autonomous nonconventional climbing robots is very important from different points of view: integrity of the infrastructure, safety of the human operators, quality of the inspections and increment of the periodicity of inspection.^[1]

A climbing robot should not only be light, but also possess a large payload capacity, so it can carry the necessary tools. A major issue in the design of these devices is their adhesion mechanism, because unlike ground robots, climbing robots need to be self-supported in the environment without stable connection to the floor. They can be in horizontal, oblique, vertical, or in upside down position.



Figure 1.1 The *REST*, a climbing robot intended for welding in ferromagnetic walls.^[2]

When the surface is ferromagnetic, magnets can be used to provide adhesion force. Magnetic attachment is highly desirable due to its inherent reliability [2]. The evolution of these magnetic holders has been made possible by the discovery of new magnetic materials and their continual improvement. Coils, electromagnets or permanent magnets have been extensively used as attachment mechanism.

Sometimes, or the application of climbing robots, it is necessary to control the magnetic force, or at least to switch the magnetic adhesion on and off.

For this purpose electromagnets can be used. An electromagnet is a type of magnet whose magnetic field is produced by electric current. However, there are two main problems for the application of electromagnets in climbing robots. First of all, electromagnets require constant power feed to either stay on or off.

The second problem of electromagnets is that they are extremely sensitive to the air gaps and the thickness of the material. In Figure 1.2 we present a comparison between the data of an electromagnet found on a manufacturer catalog^[4] and the values given by Equation 2.1.

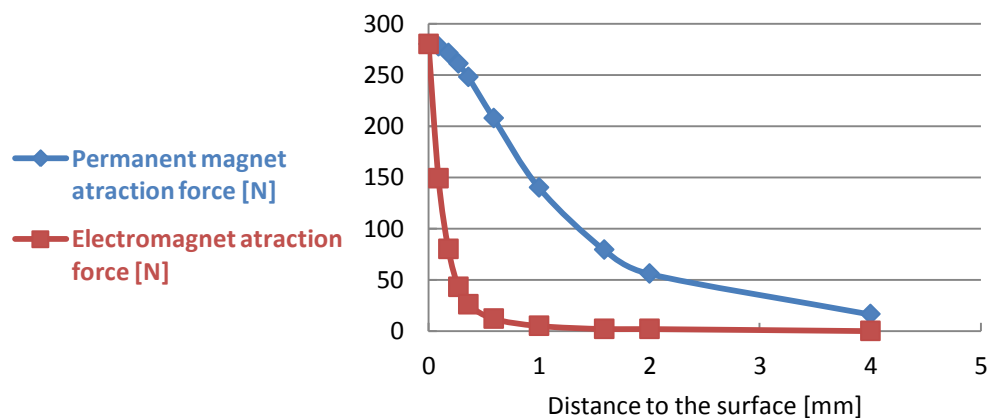


Figure 1.2 Comparison between the effect of the distance to the surface between permanent magnets and electromagnets.

On the other hand, switchable magnets only require to be powered or actuated to switch their state. If they are used like holders, they are switched manually. But if these devices are coupled with an actuator, their on/off state can be remotely controlled and can be programmed.

In spite of being used for many years in industrial applications, switchable magnets received less attention in the scientific community. There is very few research and

publication and very little information on their working principle and their design principles.

Regarding the advantages of switchable magnets, we set out several goals for this research work, which include:

1. Understanding the working principle of different types of switchable magnets;
2. Understanding the design parameters of switchable magnets, such as geometry and material of the housing;
3. Learning how to simulate and optimize switchable magnet units;
4. Designing and developing a switchable magnet unit with the highest attraction force to mass ratio since light-weight devices are desired for climbing robots;
5. Actuating the developed switchable magnet unit, in order to remotely control its state;
6. Applying and testing the device in two different robotic applications.

2. MAGNETIC HOLDING DEVICES

2.1. Introduction

Magnetic plates for retention of an attractable piece of ferrous metal are commonly used in surface grinding and other machines. They are preferred when a mechanical gripping of the work piece is undesirable because the jaws of the vise or clamp would interfere with the machining operation or difficulties may be encountered in engaging or disengaging the structures.

In this chapter we begin to analyze different types of the simplest magnetic device, the permanent magnet. For that purpose we need to understand some physical concepts, which are explained. Then we have again physical explanations, this time about electromagnets, and it is not necessary to describe the different types of components, because, apart from the dimensions, their working principle is the same.

Then we discuss electropermanent magnets, a relatively new concept that is beginning to be used on some small robotic applications, and different models of this device are presented.

Finally, we set to analyze switchable magnets, their different possible configurations and some robotic applications. Information about the *MagJig 95* model range, which we will analyze in the next chapter, is also provided.

2.2. Permanent magnets

2.2.1. Physical background

Ferromagnetic materials are composed of microscopic regions called magnetic domains that act like tiny permanent magnets that can change their direction of magnetization. Before an external magnetic field is applied to the material, the domains are oriented in random directions. Their tiny magnetic fields are oriented in random directions and cancel each other out, so the material has no significant magnetic field. When an

external magnetizing field (H) is applied to the material, it aligns the domains, causing their tiny magnetic fields to turn and align parallel to the external field, adding together to create a large magnetic field which extends out from the material (B). This is called magnetization. The stronger the H , the more the domains align yielding a higher B .

As can be seen in Figure 2.1, this magnetization as a function of the external field is described by a hysteresis curve. Starting at the origin, the upward curve is the initial magnetization curve. The downward curve after saturation, along with the lower return curve forms the main loop.

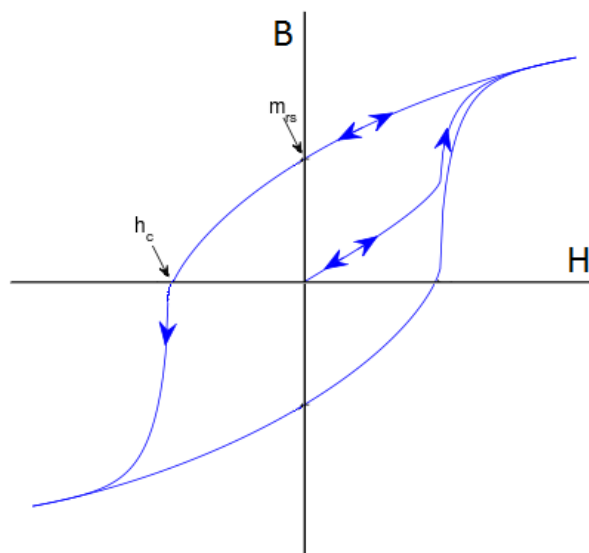


Figure 2.1 Magnetic hysteresis, in which B is the magnetization of the material, H the magnetic field, m_{rs} the remanence and h_c the coercivity.

The remanence (m_{rs}), is the magnetic flux density remaining in a magnetized body when, the applied magnetic field strength is brought to zero and is half of the height of the middle section of the hysteresis loop. The coercivity (h_c) is the intensity of a magnetic field required to reduce the magnetization of a material to zero after the magnetization of the sample has been driven to saturation and is half of the width of the middle section. A higher coercivity increases the ability of a magnet to withstand negative or alternating fields without changing its behavior.

As the H field increases, the B field approaches a maximum value asymptotically, the saturation level for the substance. It occurs when practically all the domains are lined up, so further increases in H is not able to considerably increase B . Technically, above

saturation, the B field continues to increase, but at the paramagnetic rate, which is three orders of magnitude smaller than the ferromagnetic rate seen below saturation.

The maximum energy product (also referred as BHmax) of a magnet is an energy density. This means that magnets with different dimensions made from the same material will have the same maximum energy product, although they create different magnetic fields. It is equivalent to the area of the largest rectangle that can be inscribed under the hysteresis curve (Figure 2.2).

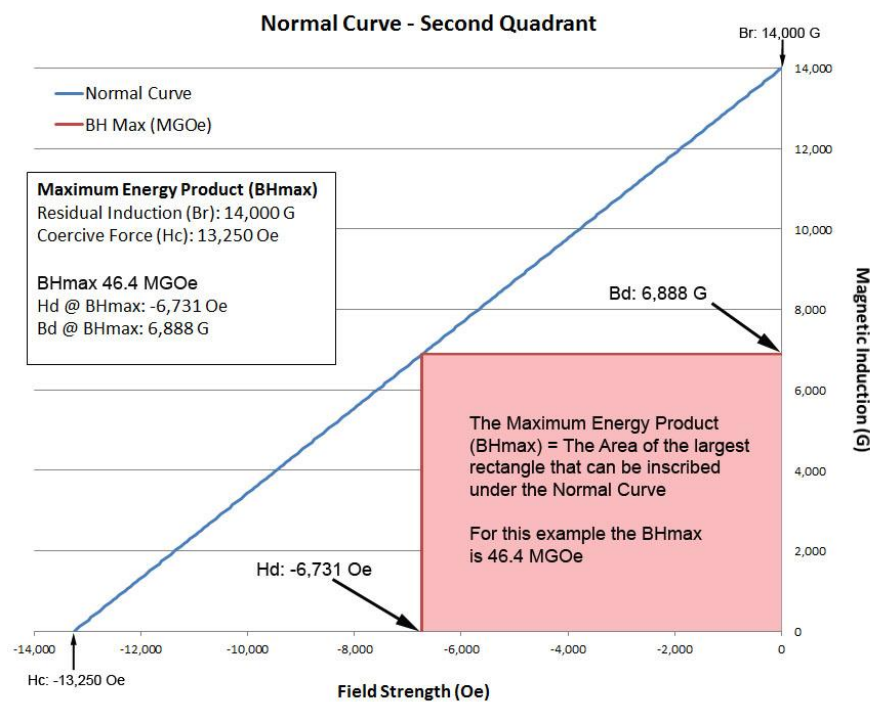


Figure 2.2 Maximum energy product of a magnet. ^[6]

A permanent magnet is an object made from a material that is magnetized and creates its own persistent magnetic field. They are made from materials with high remanence and high coercivity, which are hard alloys with many defects in their crystal structure where the domain walls hold and stabilize.

The Curie temperature is the critical point where a material's intrinsic magnetic moments change direction (Figure 2.3). Magnetic moments are permanent dipole moments within the atom which originate from electrons angular momentum and spin.

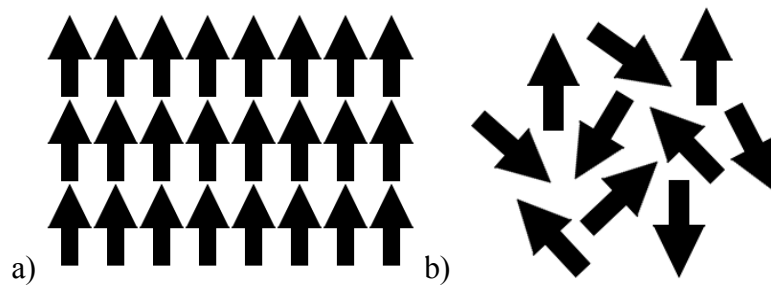


Figure 2.3 Effects of Curie temperature: a) Below the Curie temperature, neighbouring magnetic spins align^[8], b) Above the Curie temperature, the magnetic spins are randomly aligned^[9].

Magnets can be demagnetized by heating a magnet past its Curie temperature; the molecular motion destroys the alignment of the magnetic domains. This always removes all magnetization, even after cooling below that temperature.

2.2.2. Magnetic force

When imposed to a ferromagnetic structure (Figure 2.1), the permanent magnet attraction force decreases greatly with the distance to the surface. This relation is described in Equation 2.1.^[7]

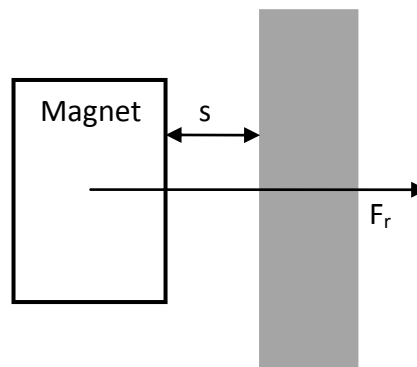


Figure 2.4 Magnet at a distance s from the surface.

$$F_r = \frac{F_h}{1+s^3} \quad (2.1)$$

Where:

- F_r is the magnetic force at distance s ;
- F_h is the maximum magnetic force of magnet in contact with surface;
- s is the distance between the surface and magnet.

2.2.3. Types

Ceramic magnets

Also known as ferrite magnets, they are made of a composite of iron oxide and barium or strontium carbonate. These materials are only desirable due to their lower cost. The resulting magnets are non-corroding but brittle and must be treated like other ceramics.

Alnico magnets

Alnico magnets became popular around the 1940s and are made up of a composite of aluminum, nickel and cobalt with small amounts of other elements added to enhance the properties of the magnet. Alnico magnets have good temperature stability, good resistance to demagnetization due to shock but they are easily demagnetized because their coercivity is low.

Samarium cobalt magnets

The rare earth elements are metals that are ferromagnetic, meaning that like iron they can be permanently magnetized, but their Curie temperatures are below room temperature, so in pure form their magnetism only appears at low temperatures. However, they form compounds with the transition metals such as iron, nickel, and cobalt, and some of these have Curie temperatures well above room temperature. Rare earth magnets are made from these compounds. The advantage of the rare earth compounds over other magnets is that their crystalline structures have very high magnetic anisotropy. This means that a crystal of the material is easy to magnetize in one particular direction, but resists being magnetized in any other direction.

Introduced into the market in the 70's, samarium cobalt is a type of rare earth magnet material that is highly resistant to oxidation, has a higher magnetic strength and temperature resistance than alnico or ceramic magnets. Due to the high cost of samarium, samarium cobalt magnets are commonly used for applications where high temperature and corrosion resistance is critical.

Neodymium magnets

Developed in 1982 by General Motors and Sumitomo Special Metals, they are the strongest and most affordable type of rare-earth magnet. This material has similar

properties as the samarium cobalt except that it is more easily oxidized and generally doesn't have the same temperature resistance. Because they are highly corrosive in many commercial products a protective coating is added to prevent exposure to the atmosphere. Nickel plating or two-layered copper-nickel plating are the standard methods, although plating with other metals, or polymer and lacquer protective coatings are also used.

The most relevant values for each type of magnet were taken from a magnets manufacturer^[10] and are presented on Table 2.1.

Table 2.1. Comparison between each type

	Remanence [T]	Coercivity [kA/m]	Maximum energy product [kJ/m ³]	Curie temperature [°C]
Ceramic	0.2–0.4	150–200	8–34	450
Alcino	0.7–0.9	45–160	13–72	700–860
Samarium cobalt	0.8–1.2	413–835	110–240	720
Neodymium	1.0–1.4	800–1100	220–360	310–400

2.3. Electromagnets

Permanent magnets suffer from the drawback that their energy output is fixed and they cannot be employed if a variation in magnetic field strength is required. To solve this problem, it has been customary to control magnetic fields by using electromagnets.

An electromagnet is a type of magnet in which the magnetic field is produced by electric current, which flows through a wire and creates a magnetic field around it, due to Ampere's law.

2.3.1. Physical background

The Ampere's circuital law was discovered by André-Marie Ampère in 1826 and relates the integrated magnetic field around a closed loop to the electric current passing through the loop.

$$\oint_C B \, dl = \mu_0 \iint_S J \, dS \quad (2.1)$$

Where:

- \oint_C is the closed line integral around the closed curve C;
- B is the magnetic field around the wire;
- μ_0 is the vacuum permeability;
- \iint_S is the 2d surface integral over S enclosed by C;
- J is the total current density.

In a practical way, this means that current (I) through a wire produces a magnetic field (B) around it (Figure 2.5). The magnetic field lines of a current-carrying loop of wire pass through the center of the loop, concentrating the field there.

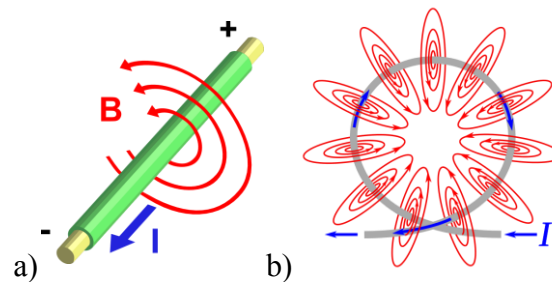


Figure 2.5 Effects of Ampere's circuital law: a) magnetic field created around a wire^[11], b) created around a loop.^[12]

To concentrate the magnetic field, in an electromagnet the wire is wound into a coil with many turns of wire lying side by side. The magnetic field of all the turns of wire passes through the center of the coil, creating a strong magnetic field there.

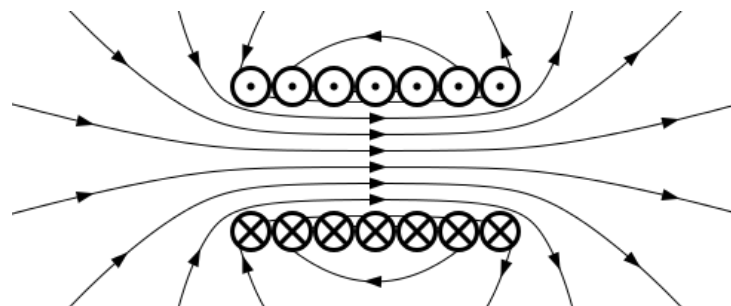


Figure 2.6 Magnetic field created around a solenoid.^[13]

The intensity and orientation of the magnetic fields of electromagnets can be successfully adjusted by controlling the strength and direction of the electric current. The magnetic field disappears when the current is turned off.

Electromagnets are widely used to provide variable-intensity magnetic fields as components of other electrical devices, such as motors, generators, relays, loudspeakers, hard disks, MRI (magnetic resonance imaging) machines, scientific instruments, and magnetic separation equipment, as well as being employed as industrial lifting electromagnets for picking up and moving heavy iron objects like scrap iron.^[14]

While electromagnets have wide application, they are generally expensive to manufacture. Also the electromagnetic forces produced by coils and electromagnets strongly depend on energizing coil Ampere turns, thus inevitably causing problems, such as high power consumption, high temperature, potential safety hazard, short service life, heavy weight and high maintenance cost.^[15]

Other problem is that a certain amount of leakage of magnetic energy is present at the non-magnetic gaps when the devices are in off or nonmagnetic positions. Therefore, electromagnets are not best suited for use in connection with sensitive electrical equipment because of possible interference resulting from the magnetic leakage.

2.4. Electropermanent magnets

These devices are a combination of a permanent magnet (used to generate the magnetic force for attracting the object) and an electromagnet (used to neutralize the permanent magnet).

The energized state may be established by the application of an electrical pulse of proper magnitude and sufficient duration to retain the work piece by the magnetic forces of permanent magnets and without further electrical supply. The application of a reverse pulse can, however, nullify the magnetic field to permit the work piece to be removed from the magnetic holder. Thus, electropermanent magnets give the functionality of electromagnets, which can be switched on and off, to permanent magnets.

2.4.1. Types

Magnetic Plate

It was patented in 1978 by Philibert Maurice Brailion.^[16] Its permanent magnets are ceramic, so they have a higher coercivity than its electromagnets, which have a core made from alnico (Figure 2.7).

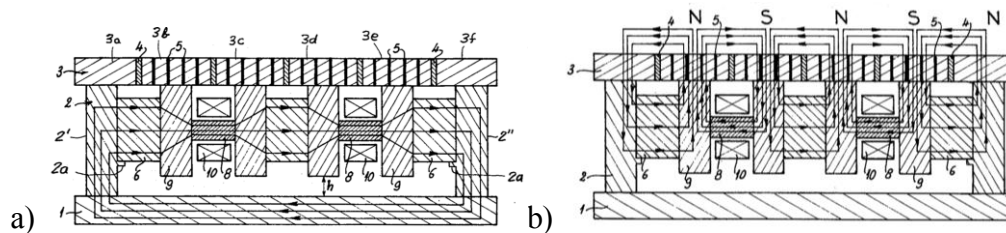


Figure 2.7 Operation of a magnetic plane: a) off state: the low coercive magnets 8 were magnetized in the same direction as the high coercive magnets 6 by the passage of an electrical pulse through the coils 10 in a suitable sense, b) on: the magnets 8 have their magnetic fields established opposite to that of magnets 6 by the pulsed energization of coils 10 in the opposite sense.^[16]

Parallel electropermanent magnets

It is made from the parallel combination of neodymium and alnico magnets. A current pulse in the coil switches the device between the on and off states, by switching the magnetization of only the alnico magnet, which has a lower coercivity than the neodymium magnet.

A positive current pulse through the coil results in a clockwise flux through the magnet and keeper, magnetizing the alnico magnet rightward, turning the device on. When the magnet is on, the neodymium and alnico magnets are magnetized in the same direction, so that the magnetic flux travels outside the device and through the target, attracting it to the magnet. A negative current pulse imposes a counterclockwise flux through the magnet and keeper, magnetizing the alnico magnet leftward, turning the device off. When the device is in the off-state, the neodymium and alnico magnets are oppositely magnetized, so the flux circulates only inside the device. (Figure 2.8).

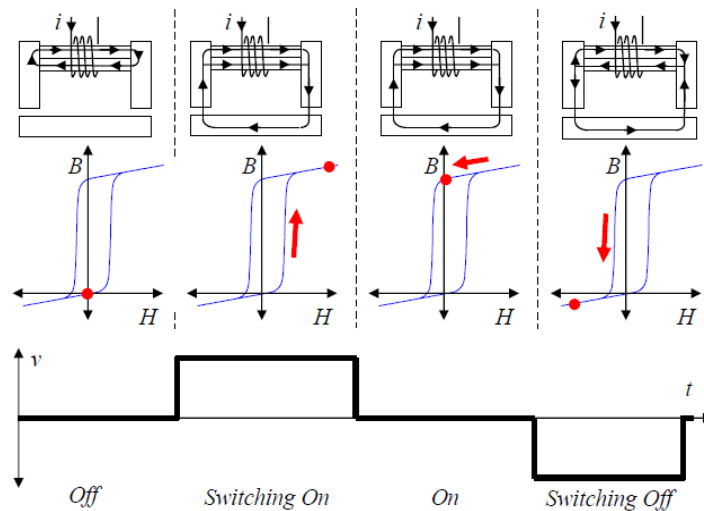


Figure 2.8 Operation of a parallel electro permanent magnet.^[17]

2.5. Switchable magnets

Switchable magnets are magnetic devices that are activated and deactivated by a mechanical rotation of one their components. The first use of this device used a rotor that switched on or off a magnetic circuit. However, nowadays the phase shift is usually accomplished by moving a circular permanent magnet.

Comparing with electromagnets, switchable magnets with the same weight:

- Consume less energy;^[18]
- Have a higher adhesion force;^[18]
- Are not compromised by lack of energy;
- Are economically designed and manufactured;
- Increase battery life, because they are not always using it;
- Can be completely turned off;^[19]
- Are less sensitive to distance.

2.5.1. Types

Neptune magnetic holder

The Neptune robot^[22], whose design is detailed further in the next section, uses a switchable magnet which works like a circuit. It consists in a metallic shaft that can be turned in order to open or close a magnetic circuit, causing the magnetic flux to go around

the magnet resulting in the absence of magnetic attraction or through the resting surface with the magnetic holding effect. However, as we can see on Figure 2.9 there is still some leakage on the off state.

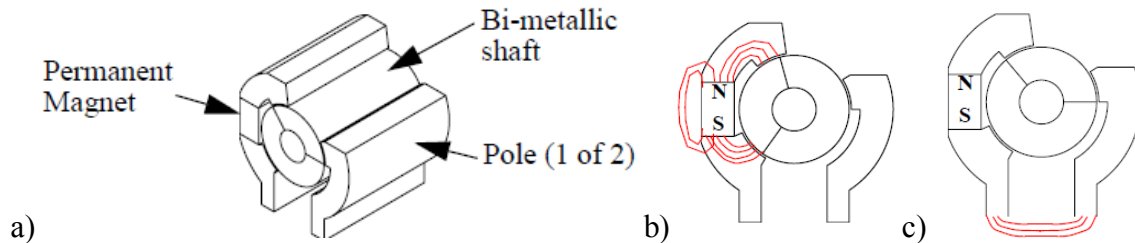


Figure 2.9 Neptune magnetic holder: a) configuration, b) off state, c) on. ^[22]

Variable magnet

In 1965 Bey Ahmet K. patented a switchable magnet that uses a flux neutralizations principle instead of the circuit approach. ^[19] It comprises a sleeve made from a permanent magnet, in which pole pieces are secured on opposite sides, and a diametrically magnetized cylindrically-shaped magnet rotatable within the sleeve (Figure 2.10).

The torque required to turn the magnets depends on the external ferromagnetic circuit. It is the highest if the system is activated in the air and the lowest if there is a ferromagnetic plate in direct contact.

Even in the off position, there is a slight magnetic leakage which would render the device unsuitable for use with some electrically actuated components. To completely stop it, a magnetic leakage stopper is provided, which is fabricated from a magnetizable material, such as soft iron or other ferrous material.

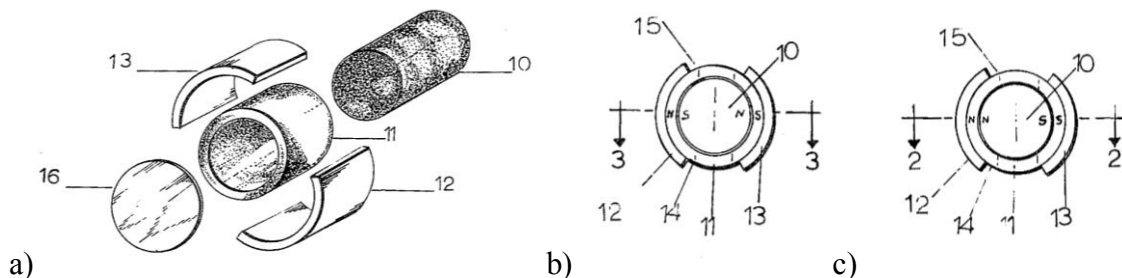


Figure 2.10 Variable magnet: a) configuration, b) off state: when the device is off, the north magnetic area of the surface of core is coincident with the south magnetic area of the inner surface of the sleeve 11, c) on: as the core 10 is rotated with respect to the sleeve 11, the flux travels between the opposite poles that are getting apart between each other's and the magnetic fields are increasing until, at 180 degrees, the magnet is on. ^[19]

Turn-off Permanent Magnet

Arlo F. Israelson, patented this device in 1969.^[20] It contains two permanent magnets, sandwiched between two pole pieces. One of the permanent magnets is fixed but the other can be rotated using a crank (Figure 2.11).

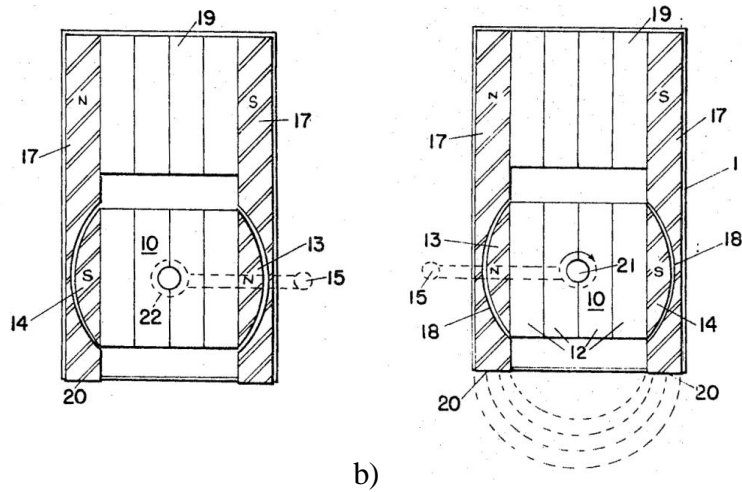


Figure 2.11 operation of a magnetic plane: a) off: with both magnets facing opposite directions aligned, the device is off, b) on: rotating the crank aligns the magnets, making the magnetic flux circulate outside the device only.^[20]

H-type

One simple configuration of a switchable magnet is known as H-type and is composed by a stator and a rotor (Figure 2.12). The rotor is a diametrically magnetized cylindrical magnet which turns along an axis parallel to the adhesion surface. It turns between two u-shaped iron pieces forming the stator.

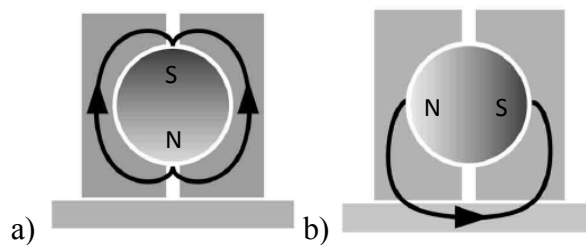


Figure 2.12 Operation of an H-type device: a) off: all the flux goes between the poles through both u-shaped iron parts, b) on: by turning the magnet by 90° degrees, the flux goes from North Pole through one u-shaped iron, through the plate and the second u-shaped iron to the South Pole.^[18]

H-type double magnets

In 2006 Perry J Underwood and Franz Kocijan registered a device containing two cylindrical permanent magnets.^[21] Turning the upper magnet causes its magnetic field to neutralize or to add to the magnetic field of the lower magnet (Figure 2.13).

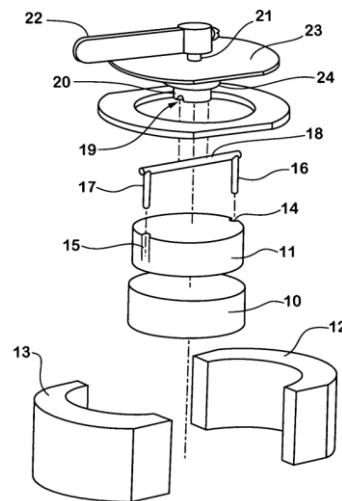


Figure 2.13 Configuration of a H-type double magnets device^[21].

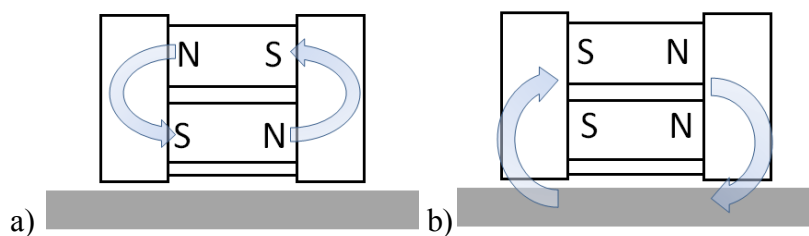


Figure 2.14 Operation of a H-type double magnets device: a) off state: the north pole of the upper magnet overlies the south pole of the lower, so the magnetic flux travels from one magnet to another inside the device, b) on: rotating the upper magnet 180° about its axis of rotation brings the magnets into the alignment and the magnetic flux follows a path outside of the device.

2.5.2. Applications in robotics

In spite of several uses of switchable magnets in industrial environments, their application in robotics is rather new. Here we discuss two different applications: the *Neptune*, which was the first robot to use this concept, and the *Miche*, that uses a device similar to the one we propose to analyze. It seems that switchable magnets, along with electropermanent magnets start to being used in highly complex systems where one of their most important features is their miniaturization.

Neptune

The first known use of this type of magnetic holders in mobile robotics is on the Neptune robot^[22], which is a mobile robot system used to remotely inspect above-ground storage tanks while immersed in the petroleum product, in order to ascertain from the inside-out the state of corrosion of the floor and side-walls using video and ultrasonics. The magnets used in this device were described on Chapter 2.4.1.1.

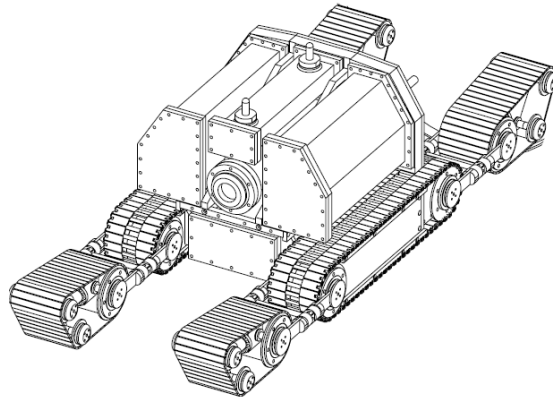


Figure 2.15 Crawler of the *Neptune* ^[22]

Miche

The *Miche* robots behave as programmable matter, which means that, starting from an amorphous arrangement, they can be assembled into arbitrary shapes and then commanded to self-disassemble in an organized manner, to obtain shape chosen by its user. This is done by eliminating the unnecessary modules from the structure in a controlled mode.

Individual actuated modules attach to each other using a switchable magnet on their sides, driven by a miniature motor with an integrated planetary gear box. The model of the magnetic device is a small custom *MagJig*, the same type of device this work proposes to analyze.

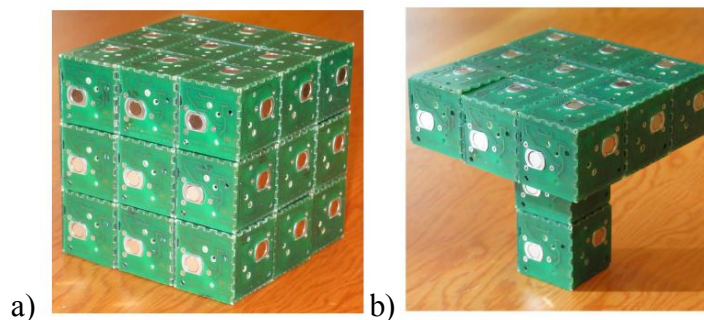


Figure 2.16 *Miche* robot: a) initial configuration, b) possible alignment. ^[23]

2.5.3. MagJig 95

In our work we study an H-shaped double magnets (Figure 2.17), usually used in holding plates in woodworks for safety, made by *Magswitch*^[24]. We chose this model due to its use in another robotics application, like the *Miche*, and its low weight, essential for being used in a climbing robot. As so, our starting basis will be the lightest of the range, which has an advertised holding force of 423 Newton.



Figure 2.17 Model range of the *MagJig* models from *Magswitch* (the model number relates to the holding force in pounds).^[24]

To establish a relation between their weight and their holding force, we need to know how much the device (consisting on the housing and the magnets) weights. So we present in Table 2.2 the total weight (including the handle) and the partial weight (just of the magnetic section) of each model.

Table 2.2. Comparison between each model

Holding force [lbs]	Holding force [N]	Total weight [g]	Partial weight [g]	Holding force per mass unit [N/g]
95	423	131	89	4.75
150	667	237	161	4.14
230	1050	450	306	3.43

In Figure 2.18 we present a graphical interpretation for this data according to the weight of each model.

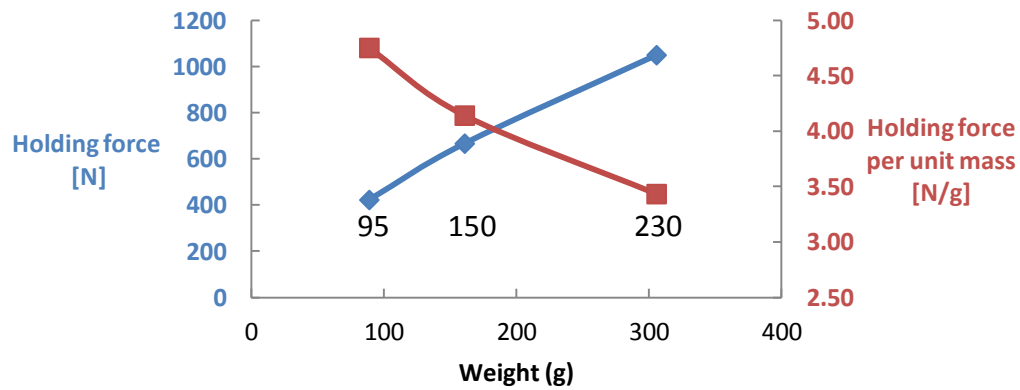


Figure 2.18 Holding force and holding force per unit mass

In this chapter we compared some of the different types of magnetic devices. We finally chose a commercial H-type double magnets device for further studies. In the next chapter we will take the *MagJig 95* as reference and will try to simulate its holding force.

3. SIMULATION

3.1. Introduction

We first try to simulate the *MagJig 95* magnets in *Comsol Multiphysics 4.3* with the *AC/DC Module* ^[25], in order to verify the validity of our model. To do so, we first developed a 3D CAD model of the *MagJig 95* and simulated it without modifications in respect with the commercial device.

Then, we introduced a series of modifications to see their effect in the magnetic holding force. That way, we can have a better understanding of the behaviour of this device and know if we should change it. These simulations include effects of the housing shape, materials and dimensions.

To help us understand how the magnetic flux is conducted, we present images of its appearance depending on each modification.

3.2. Comsol Multiphysics

Comsol Multiphysics is a finite element analysis solver package for various physics and engineering applications. It is composed of several simulation modules, such as the *AC/DC Module*. This module is used for simulating electric, magnetic, and electromagnetic fields in static and low-frequency applications, like capacitors, inductors, insulators, coils, motors, actuators, and sensors, with dedicated tools for extracting parameters such as resistance, capacitance, inductance, impedance, force, and torque.

The *AC/DC Module* formulates and solves Maxwell's equations together with material properties and boundary conditions. The equations are solved using the finite element method with numerically stable edge element discretization in concert with advanced solvers. The different formulations admit static, frequency-domain, and time-domain simulations. Results are presented in the graphics window through preset plots of electric and magnetic fields, currents and voltages, or as expressions of the physical quantities that you can define freely, as well as derived tabulated quantities. Material

properties are allowed to be spatially varying, time-dependent, anisotropic, and have losses. Both electric and magnetic media can include nonlinearities, such as B-H curves.

3.3. Materials defined in *Comsol*

In order to simulate a *MagJig 95* in *Comsol* we require first to build a 3D model of its housing. Then we need to define the materials of the housing, the ferromagnetic surface that acts against the switchable magnets and also the proprieties of the utilized magnet in the *MagJig 95* (Figure 3.1).

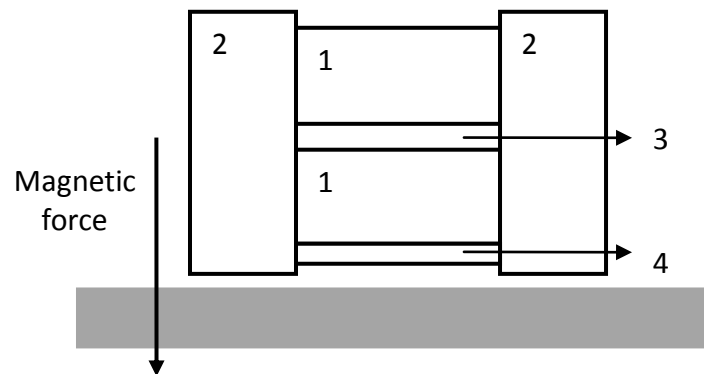


Figure 3.1 Section of the *MagJig 95*: 1) magnets, 2) housing, 3) anti-friction disc, 4) leakage stopper disc.

3.3.1. Magnets

Since we could not know exactly the grade of the neodymium magnet employed in the *MagJig 95*, we used as reference a commercially available solution with the same dimensions, from the *HKCM*^[7], a German magnets manufacturer.

One of the permanent magnet properties which the user needs to set in *Comsol* is the remanence, here referred to as flux density inside the magnet, in this case with the value of 1.38 Tesla, as can be seen in Figure 3.2.

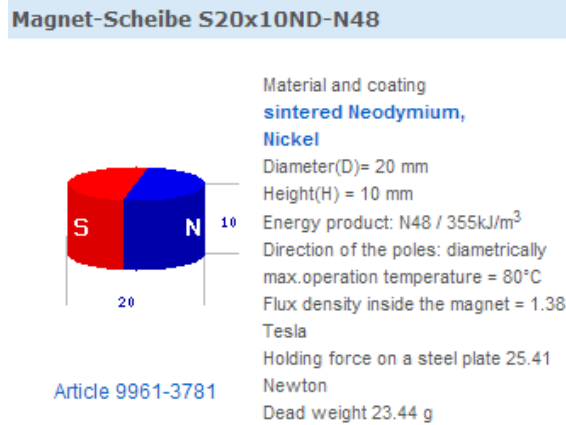


Figure 3.2 Magnet description. ^[7]

3.3.2. Housing

A model based on the *MagJig 95* dimensions was made in a CAD software and then inserted in *Comsol* (Figure 3.3).

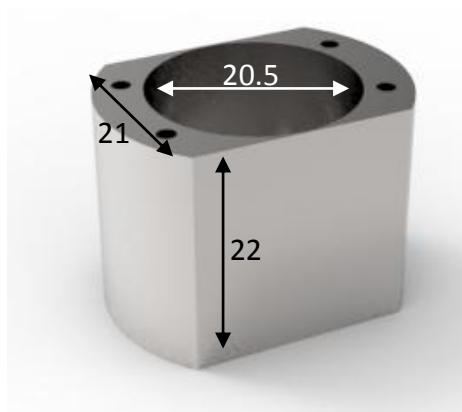


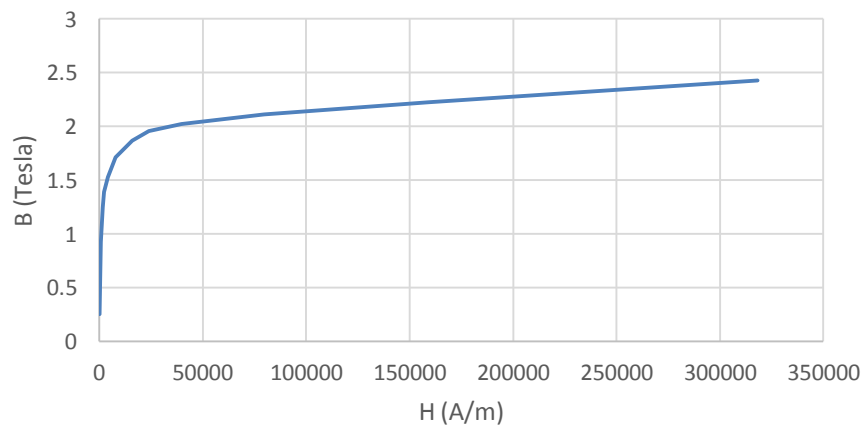
Figure 3.3 *MagJig 95* model made in a CAD software with dimensions in millimeters.

The housing in the *MagJig 95* is made from AISI 1018 metal. Its composition is described in Table 3.1.

Table 3.1. Composition of the housing metal ^[22]

Element	Content [%]
Carbon	0.14 - 0.20
Iron	98.81 - 99.26
Manganese	0.60 - 0.90
Phosphorous	≤ 0.040
Sulfur	≤ 0.050

The hysteresis curve of the housing material (Figure 3.4), provided by *Magswitch*, is very close to the one of the soft core material provided in *Comsol* database, so that material was used.

**Figure 3.4** Hysteresis curve of the housing material, provided by *Magswitch*.

3.3.3. Anti-friction disc

In the *MagJig 95* there is a plastic disc between the two magnets with the thickness of 0.1 mm. Its function is to reduce the friction and the magnetic attraction force between the magnets and to facilitate the mobile magnet rotation.

3.3.4. Leakage stopper disc

On the *MagJig 95* there is a metal disc with a thickness of 0.5 mm under the magnets to reduce the leakage. It is magnetic, so the same material as in the housing is selected.

3.3.5. Attachment plate

If the ferromagnetic plate where the magnet attaches is thicker, it will be exposed to a larger volume of magnetic field and so the holding force is bigger. The plate material that would contribute to create the bigger holding force has the lowest carbon quantity possible. Therefore, for the surface to analyze we chose a thickness of 7 mm and the same material as the housing, that it a very low carbon steel.

In the software it is placed at a distance of 0.1 mm from the magnet, because the force on the surface given by *Comsol* when there is no gap between the magnet and the surface is very small, probably due to a software limitation, so the minimum air gap possible will be considered in the software.

3.4. Simulations

After selecting the materials and modeling the geometry of the *MagJig 95* switchable magnet, we simulated its behavior in *Comsol*. We first simulated a model with properties similar to the *MagJig 95* in order to see the magnetic flux distribution and the holding force (Table 3.2). Then we tried to change parameters such as material and geometry of the housing and compare the results.

Figure 3.5 shows the section of the model housing that is visible in the simulation graphics.

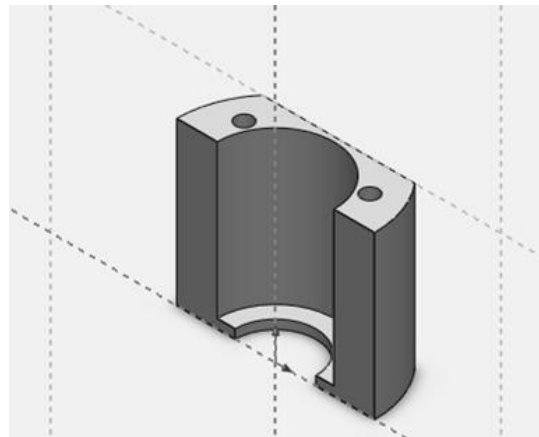
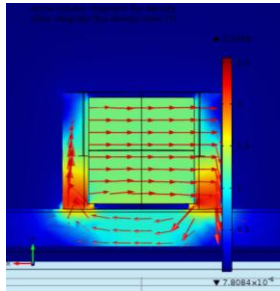
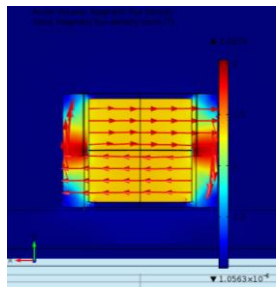


Figure 3.5 Section of the housing.

3.4.1. Simulation of the commercial device

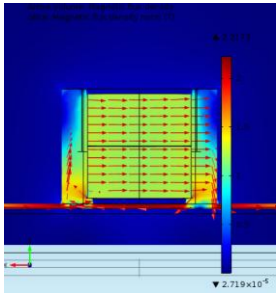
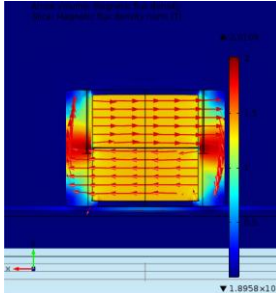
Table 3.2. Base model

	Device on	Device off
Flux density		
Holding force [N]	358.2	1.6

The flux between opposite poles goes through the surface when the device is on, and through the housing when it is off, as expected. However, the measured holding force is only of 358.2 N, while *Magswitch* claimed 423 N, a value 18% bigger than the figured. This is probably due to the gap the between the device and the surface in *Comsol*, since the distance between the materials makes a huge difference on magnetic attraction.

To compare the influence of the wall thickness, a simulation was made on an attachment plate 1 mm thick instead of the 7 mm thickness of the base model (Table 3.3).

Table 3.3. Base model on a plate 1 mm thick

	Device on	Device off
Flux density	 A 2D cross-sectional simulation showing magnetic flux density. The device is on a 1 mm thick plate. The flux is concentrated in the central region, with a maximum value of 4.9117 and a minimum of 2.719×10^{-5} .	 A 2D cross-sectional simulation showing magnetic flux density. The device is on a 1 mm thick plate. The flux is concentrated in the central region, with a maximum value of 4.9117 and a minimum of 1.8958×10^{-5} .
Holding force [N]	112.6	1.4

The force is smaller, because there is a smaller volume of the magnetic flux caught by the surface.

For comparison, the force was experimentally measured on a 1 mm steel plate. From ten tests we found an average of 87 N (77% of the simulated value) with a standard deviation of 5.0 N. This results may be explained with the wall being covered in paint and not being made of a metal as magnetizable as the introduced on the simulation.

3.4.2. Modifications

In the *MagJig 95* there is a distance of 1 mm between the bottom of the housing and the magnets, so it is interesting to test the effect of having the bottom of the magnets in the same plane as its housing (Figure 3.6).

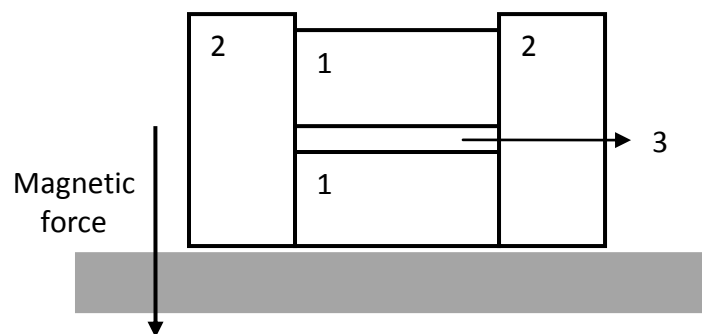
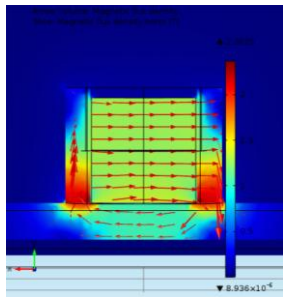
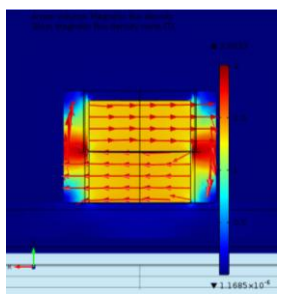


Figure 3.6 Section of the simulated device: 1) magnets, 2) housing, 3) anti-friction disc.

Table 3.4. Without air gap

	Device on	Device off
Flux density		
Holding force [N]	404.4	4.6

As we can see on Table 3.4 because the magnets are near to the surface, the force is bigger when it is on than on the base model, but when the device is off the remaining force is 187% bigger than in the original device. It is small but would offer a small opposition when the device is being detached from the surface.

Effects of the housing shape

The housing has a circular shape with two flat cuts at two sides, as can be seen in Figure 3.3. We would like to understand how this flat cut affects the device force, so we made simulations with the same dimensions that the original except for its housing being completely circular (Figure 3.7).

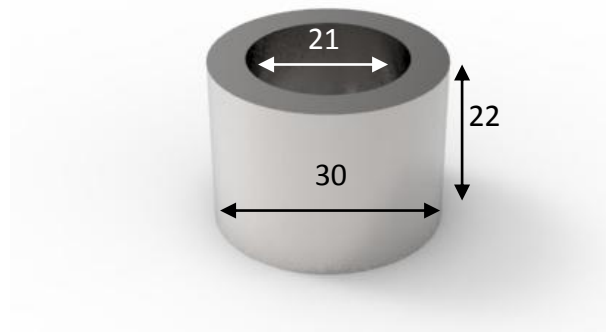
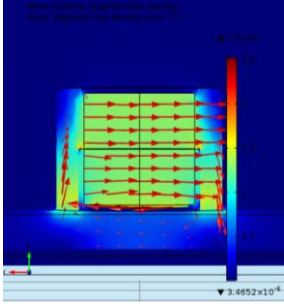
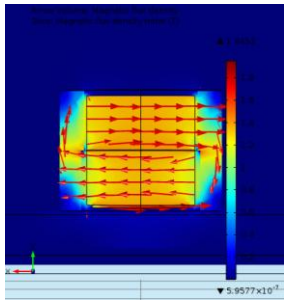


Figure 3.7 Circular housing made in a CAD software with dimensions in millimeters.

Table 3.5. Circular housing

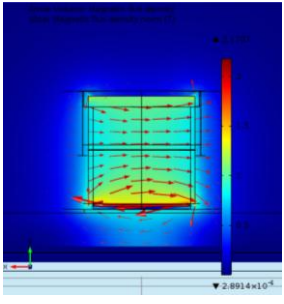
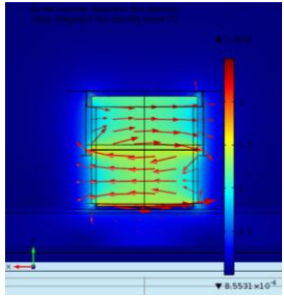
	Device on	Device off
Flux density		
Holding force [N]	86.4	1.8

After simulations, and as can be seen in Table 3.5, the holding force is much smaller, because all the magnetic flux passes through the housing, and thus it does not pass through the ferromagnetic object that should be grasped. This shows that the flat cutting has an important role in the behavior of the device.

Effects of materials

Keeping in mind that the purpose is to have a device with the least weight possible, a housing made of plastic was tested (Table 3.6).

Table 3.6. Plastic housing

	Device on	Device off
Flux density		
Holding force [N]	59.7	27.2

The magnetic field is too much dispersed to the surroundings, so there is no significant amount concentrated around the area where the soft core meets the surface.

A housing was made in a CAD software to be printed on plastic (Figure 3.8) for experimental testing. The thickness of the side walls of the original model is just 0.25 mm, but that device is made from steel, which is much stronger than plastic, so the thickness of the walls was increased to 3 mm.

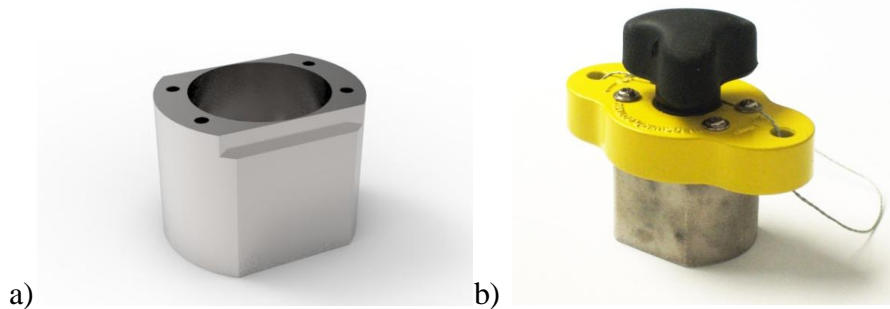


Figure 3.8 Plastic housing: a) CAD model, b) assembled.

Because we don't have a 7 mm thick wall to test the device, we had to make a simulation in *Comsol* of his behavior on a 2 mm wall to compare with the actual 2 mm steel wall we had for the tests (Table 3.7).

Table 3.7. Comparison between simulation and practical experiment

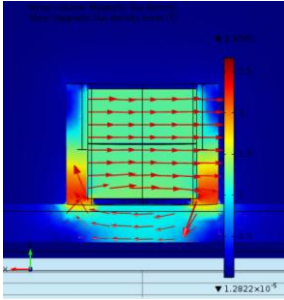
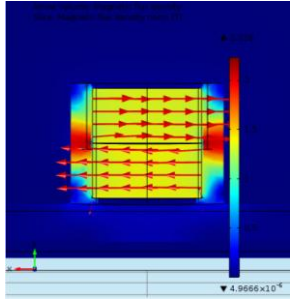
	Simulation in <i>Comsol</i>	Practical experiment
Holding force [N]	58.8	20

This difference probably is due to the material where we tested the magnets not being so magnetizable, been covered in paint and also some bending component during the applied pull force.

Effect of dimensions

Other way to reduce the weight of the device is to reduce its dimensions. So, smaller diameters were tested. In the first case, we tested an outer diameter of 28 mm, 2 mm smaller than the original.

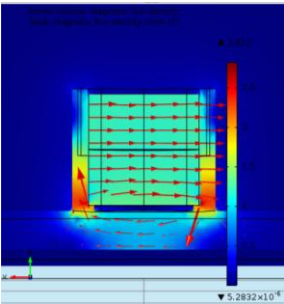
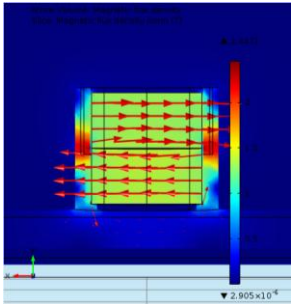
Table 3.8. Diameter of 28 mm

	Device on	Device off
Flux density		
Holding force [N]	295.8	6.44

In this case the holding force is 17% smaller than on the actual device. A simulation can be made to see the results if what happens if the outer diameter is even smaller, with 26 mm.

In this case the holding force is 32% lower than on the *MagJig 95* simulation (Table 3.9).

Table 3.9. Diameter of 26 mm

	Device on	Device off
Flux density		
Holding force [N]	240	21.7

Based on Table 3.10 we can conclude that this device is already optimized, because our modifications produced worst results than the original features.

Table 3.10. Comparison between the simulations

	Holding force (on) [N]	Holding force (off) [N]
Base model	358.2	1.6
Without air gap	404.4	4.6
Circular housing	86.4	1.8
Plastic housing	59.7	27.2
Diameter of 28 mm	295.8	6.44
Diameter of 26 mm	240	21.7

4. A NEW OPTIMIZED SWITCHABLE MAGNET

4.1. Introduction

The *OmniClimber* is an omnidirectional climbing robot for inspection of ferromagnetic structures equipped with a mechanism which enables it to perform perpendicular plane transitions (Figure 4.1).

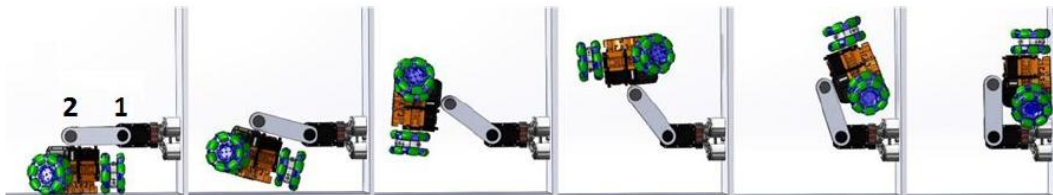


Figure 4.1 *OmniClimber VI* transition mechanism. [27]

While performing the plane transition, the magnetic attachment unit should withstand the weight of the robot and also the torque resulting from the total length of the arm. The magnetic attachment unit is composed by one central round permanent magnet with a diameter of 20 mm and three electromagnets with a diameter of 30 mm (Figure 4.2).

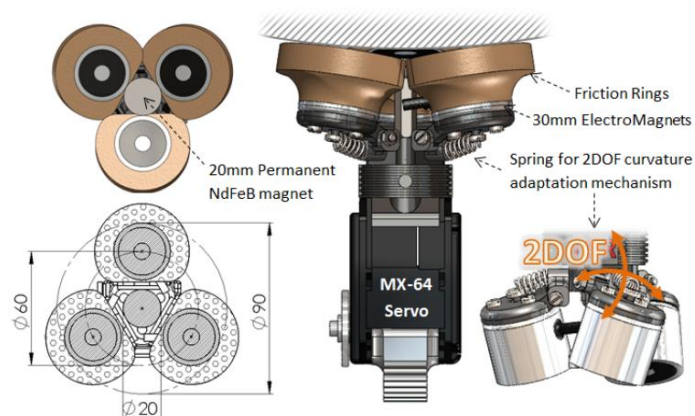


Figure 4.2 *OmniClimber* support with electromagnets. [27]

The electromagnets only need to be activated during the plane transition and are turned off during the normal operation. When the magnetic attachment unit is being used during the plane transition, the permanent neodymium magnet provides 32 N of adhesion force. In the catalog the holding force of each electromagnet is said to be 280 N in optimal conditions (Figure 4.3), but in experimental conditions ^[27] (on 1 mm thick steel), it proved to be only 45 N.

Diameter mm	Standard operating voltage						Air gap mm									
	240VAC		24VDC		12VDC		0	0.09	0.18	0.27	0.36	0.59	1.00	1.59	2.00	4.00
	Product no.	Current mA	Product no.	Current mA	Product no.	Current mA	Pull force (+/- 10%) N									
25			M52172/24VDC	90	M52172/12VDC	180	150	51	22	12	8	4	2	-	-	-
30			M52173/24VDC	140	M52173/12VDC	280	280	149	80	43	26	12	5	2	2	-
40			M52174/24VDC	230	M52174/12VDC	440	550	276	144	83	57	30	14	7	5	3
50	M52175/240VA	40	M52175/24VDC	240	M52175/12VDC	470	1000	655	442	282	187	87	37	24	19	6
65	M52176/240VA	50	M52176/24VDC	340	M52176/12VDC	690	1670	1137	792	533	347	180	78	39	23	11

Figure 4.3 Electromagnet advertised force. ^[4]

We will use these electromagnet’s characteristics as a starting point to our study on the development of a switchable magnet. So, with the goal of producing roughly the same force than the electromagnets, we set to design a switchable magnet with the maximum holding force per unit mass ratio and specifically suited for climbing robots. The bending on the device should be avoided because this causes the robot to detach the surface (Figure 4.4). In this context we kept the shape of the base but decreased the length.

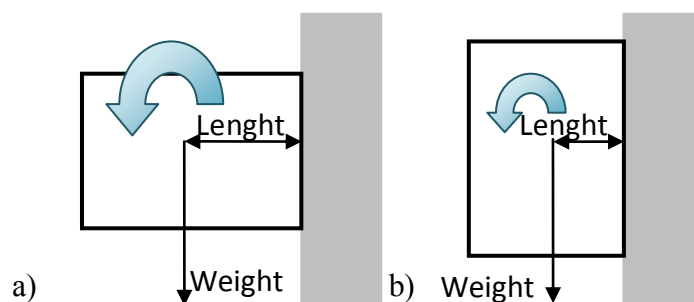


Figure 4.4 Torque resulting from different shapes of the device: a) more bending torque, b) less bending torque.

Because the dimensions of the magnets are standard we will decrease their height from 10 to 5 mm, so the novel device will be 12 mm tall.

4.2. Magnets

We need magnets similar with the ones from the *MagJig 95* but with half of the height (Figure 4.5).

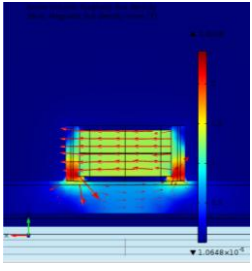
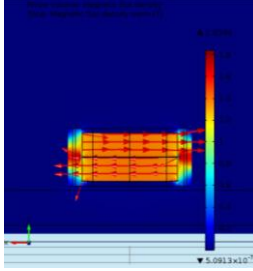
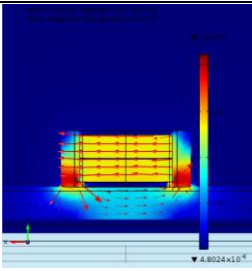
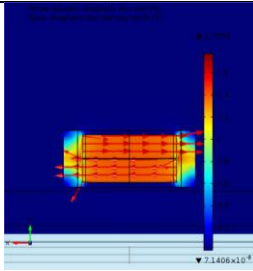
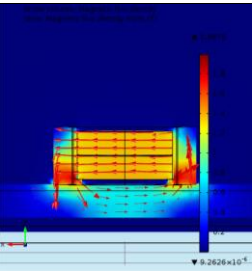
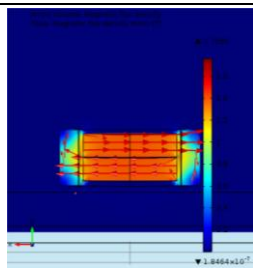
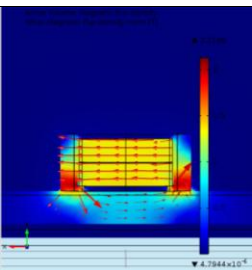
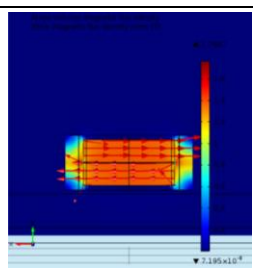


Figure 4.5 Magnet description. ^[7]

4.3. Housing

If the required height is chosen, we can compare different diameters to see their relation to the holding force. Attending that the iron density is 7.86 g/mm³, we can use *SolidWorks* to evaluate the weight of the devices. Because the goal is to have the maximum holding force/weight ratio, we need to have a relation between the force and the weight of each device (Table 4.1) and graphically represented on Figure 4.6.

Table 4.1. Comparison between each design

Outer diameter [mm]	Flux density on	Flux density off	Holding force on / off [N]	Total weight [g]	Force per unit mass [N/g]
26			165.6 / 0.1	37.6	4.4
28			190.3 / 0.1	42.1	4.5
30			191.3 / 0	46.5	4.1
32			190.2 / 0.2	50.9	3.7

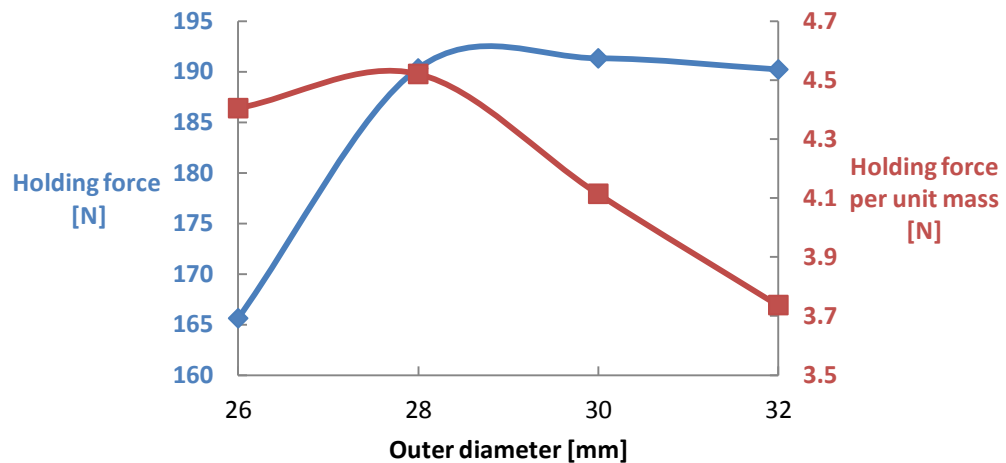


Figure 4.6 Absolute force and force per unit mass

The higher force is achieved by a housing with the same diameter of the *MagJig 95*, but the one with a diameter of 28 mm is 10% lighter and only 0.5 % weaker, so it would be the most efficient solution (the drawing is on the appendix).

Therefore we developed this device and tested it on a 1 mm thick steel plate of a locker (Figure 4.7). After 10 tests we found that the average was 56.5 N with the standard deviation of 2.6 N.



Figure 4.7 Experimental testing

To these results be suitable to be compared with *Comsol* values, we made simulations with a plate 1 mm thick (Table 4.2).

Table 4.2. Novel device on a plate 1 mm thick

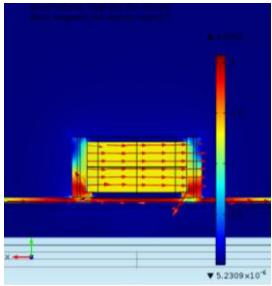
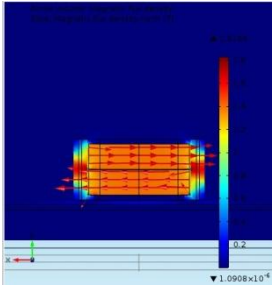
	Device on	Device off
Flux density		
Holding force [N]	100.1	0.1

Table 4.3. Comparison between the *MagJig 95* and the novel device

	<i>MagJig 95</i>	Novel device	% in relation to the <i>MagJig 95</i>
Housing weight [g]	41.7	18.1	-56.6
Magnets weight [g]	23 + 23	12 + 12	-47.8
Total weight [g]	87.7	42.1	-52.0
Holding force in <i>Comsol</i> (7 mm steel) [N]	358.2	190	-47.0
Holding force in <i>Comsol</i> (1 mm steel) [N]	112.6	100.1	-11.1
Measured holding force (1 mm steel) [N]	87	56.5	-35.1
Measured holding force per unit mass [N/g]	1.0	1.4	+9.8

With the results presented in Table 4.3 we can see that the novel device force on a 7 mm thick wall is half of the *MagJig 95* force, but on a 1 mm thick wall the force is closer between the two devices, so we can conclude that the decrease of the height causes the decrease of the amplitude of magnetic field. Because it cannot reach so far away, the increased thickness of the wall has no effect on increasing the magnetic force, whereas on *MagJig 95*, the broader magnetic field reaches a deeper area of the wall (Figure 4.8).

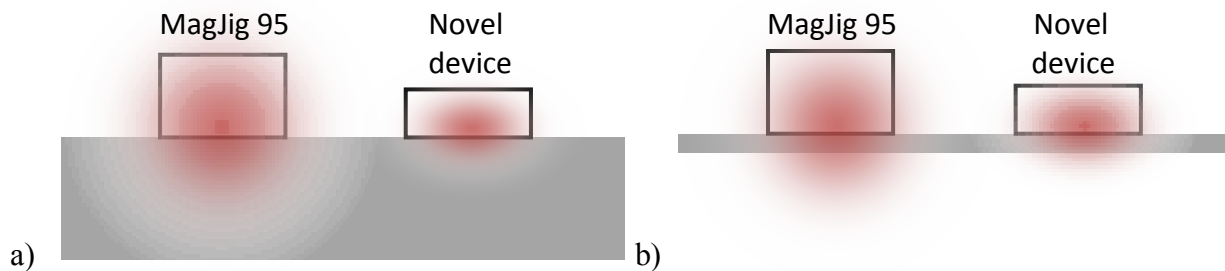


Figure 4.8 Comparison between the magnetic field of the *MagJig 95* and of the novel device: a) 7 mm thick plate, b) 1 mm thick plate.

This means that for climbing a steel plate 1 mm thick, like the ones used in air HVAC (heating, ventilation, and air conditioning) systems, a robot has not more advantages by having a tall magnetic unit, instead it would become more expensive and heavier. However, climbing robots used in the inspection of massive structures, like wind turbines, can take advantage of the magnetic adhesion potential, because by using taller magnets they can increase their weight and payload.

Finally we compare the currently used electromagnet device and the novel device in Table 4.4.

Table 4.4. Comparison between the electromagnet and the novel device

	Electromagnet	Novel device	% in relation to the electromagnet
Weight [g]	108	42.1	-61.0
Measured holding force (1 mm steel) [N]	45	58	+25.6
Measured holding force per unit mass [N/g]	0.42	1.38	+228.6

We see that it is possible to make a more compact and lighter unit compared to the electromagnet with a slightly bigger force. However, to the weight of the magnetic devices we have to add the weight of the motor needed to drive the switchable magnet, so we can compare these parameters for a unit with an actuator (Table 4.5). We chose a *Robotis Dynamixel AX-12*^[28], but, as we will see, it is possible for this motor to control at least three magnets, and we also could use a lighter motor, so this comparison was made for the worst scenario possible.

Table 4.5. Comparison between the electromagnet and the novel device with an actuator

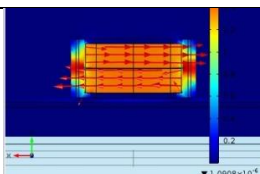
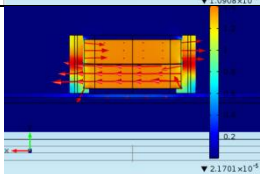
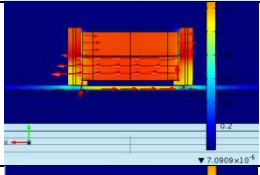
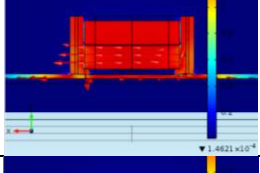
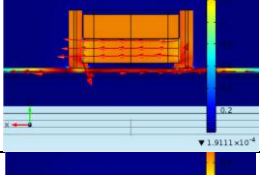
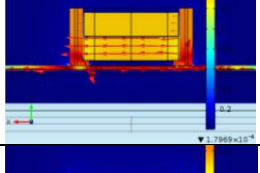
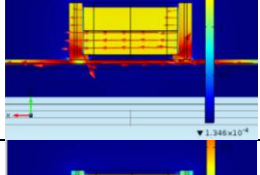
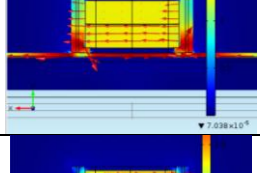

	Electromagnet	Novel device + AX-12	% in relation to the electromagnet
Weight [g]	108	97.1	-10.1
Measured holding force (1 mm steel) [N]	45	56.5	+25.6
Measured holding force per unit mass [N/g]	0.42	0.58	+38.5

Even in this case, the novel unit has a holding force per unit mass approximately 40% percent bigger than an electromagnet. Adding to the small weight of these devices, there is the reduction in energy consumption of the switchable magnets, compared to the

electromagnets, so we can clearly see advantages in the application of switchable magnets, rather than electromagnets.

To see how the force would change with the degree of rotation of the upper magnet, we made five experiments for each position on the same 1 mm thick steel (Table 4.6). This can be useful for different applications, such as reduction of the noise, because the adhesion force between the devices would be smaller and so their contact would produce a lower sound, the adjustment of the needed attraction force depending on the payload or the control of the moving velocity of the robot. We will use this feature for this last application on Chapter 6.

Table 4.6. Holding force depending on the angle

Angle between the two magnets [degrees]	Flux density	Holding Force in <i>Comsol</i> [N]	Holding force measured experimentally [N] (average of 5 experiments)
0		1.6	0
22.5		0.99	Not enough force to evaluate
45		10.6	5.4
67.5		33.9	17.9
90		58.5	26.9
112.5		77.9	39.6
135		90.9	44.7
157.5		97.8	49.8
180		100.1	56.5

In Figure 4.9 we can see the difference between these values.

$$Error = \frac{Comsol\ result - Experiment\ result}{Comsol\ result} \quad (5.1)$$

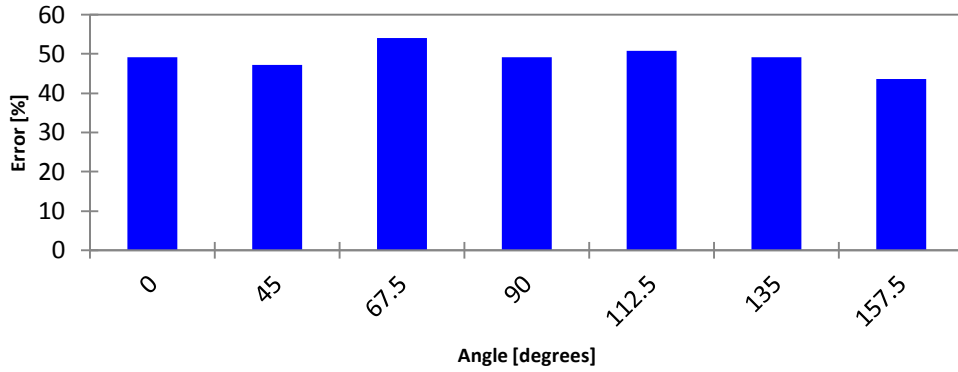


Figure 4.9 Difference between the *Comsol* results and the experiments.

The experimental force is about half of the one given by *Comsol*, which can be related to the existence of paint on the surface, different material than in *Comsol* and some sliding of the device during the tests due to bending.

Using *Excel*, we made a nonlinear regression to find a function that describes the measured holding force depending on the angle (Figure 4.10). The one that showed the best results was a polynomial of the fourth degree (Equation 5.2), with the mean square error of 0.9933.

$$y = 7^{-8}x^4 - 5^{-5}x^3 + 0.0088x^2 - 0.1552x - 0.1779 \quad (5.2)$$

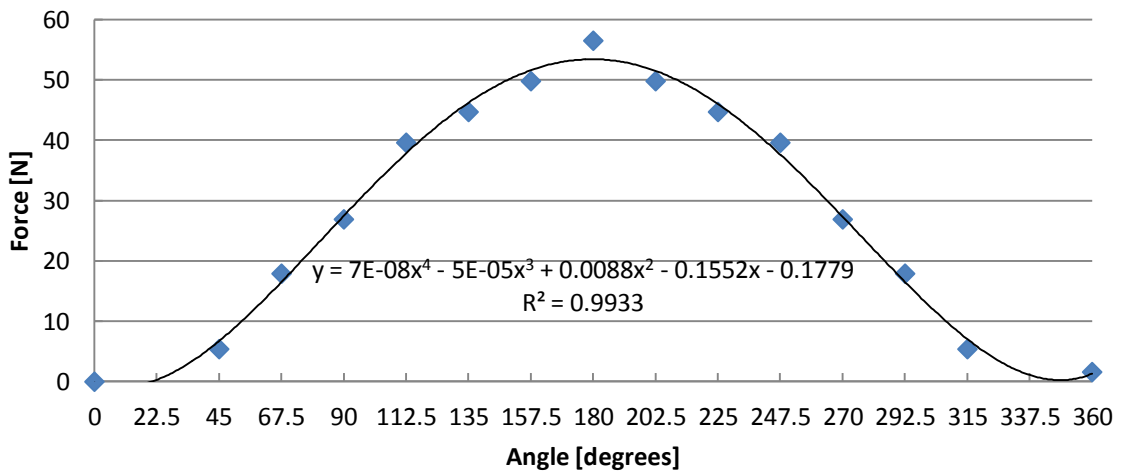


Figure 4.10 adjustment of a polynomial to *Comsol* value

5. OMNICLIMBER MAGNETIC HOLDING DEVICE

5.1. Introduction

In this chapter we describe one of the applications of switchable magnets. In this case we tried to replace the current *OmniClimber* holding device that is installed at the end of its arm (Figure 4.10) and is composed of electromagnets with a novel unit that takes advantage of switchable magnets.

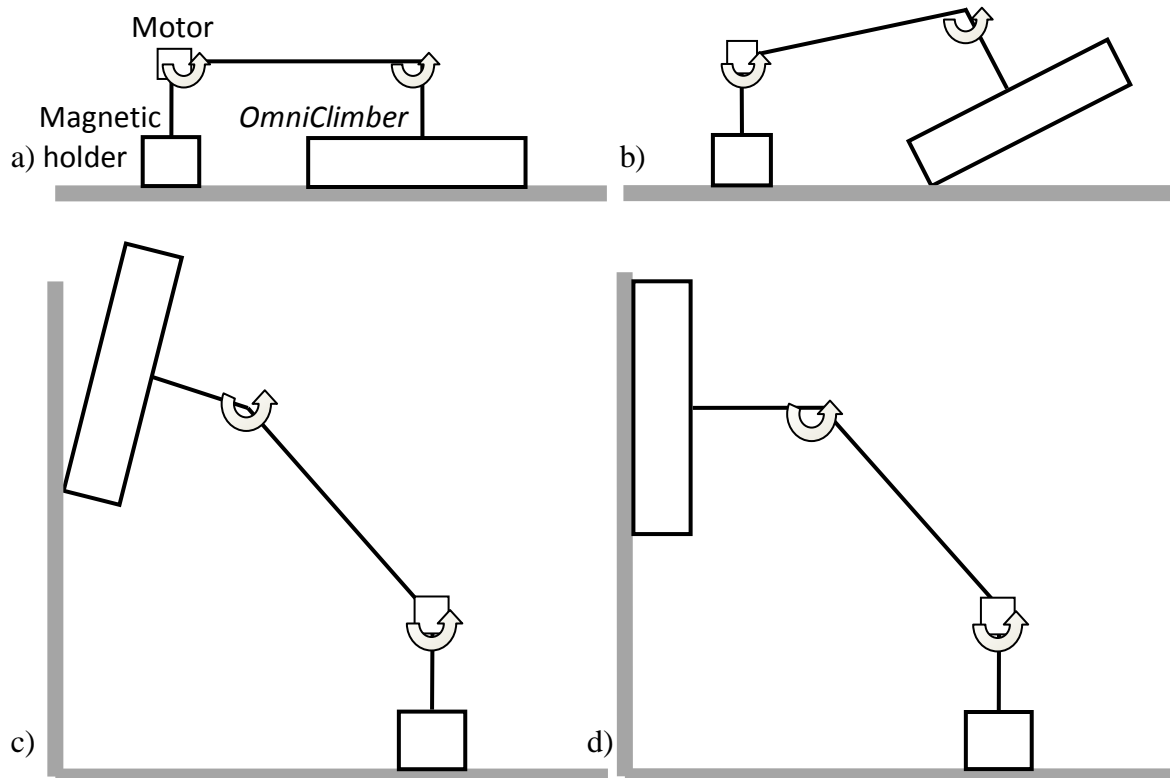


Figure 5.1 Operation of the device: a) initial position, b) the *OmniClimber* is raised, c) It reaches the surface, d) the permanent magnets makes it attach to the surface.

5.2. Design

In order to adapt to both flat and curved surfaces, the *OmniClimber* electromagnets support must guarantee two degrees of freedom for each magnetic unit. Because we want to keep the same degrees of freedom on the support with the switchable magnet, each

switchable magnet must be driven by a drive shaft. The drive shaft is composed by a universal joint at each end and a cylinder in the center (Figure 5.2).

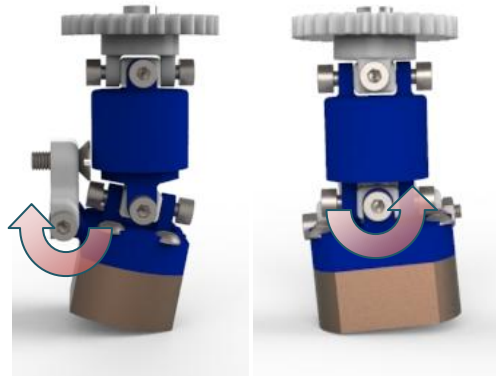


Figure 5.2 Degrees of freedom accomplished by the transmission axle of the switchable magnets.

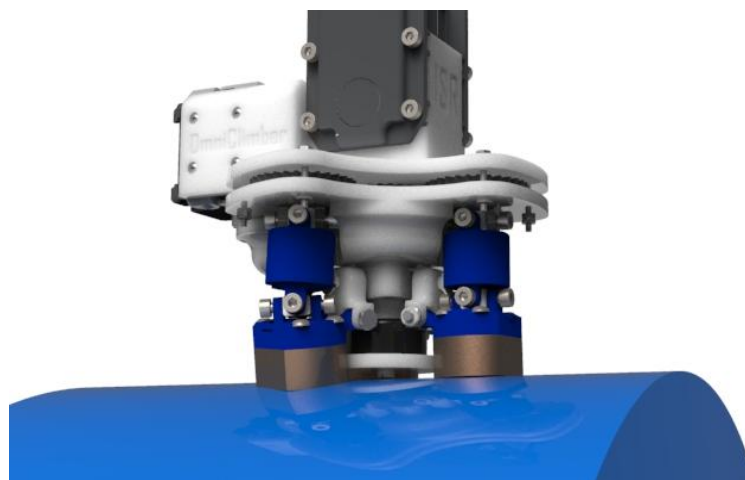


Figure 5.3 *OmniClimber* support with switchable magnets on a curved surface.

5.3. Features

We intend to use one motor to drive 3 switchable magnets. In order to do this a transmission mechanism with 2 stages was designed, to drive the rotation from one motor to each switchable magnet.

The actuator we chose is a *Robotis Dynamixel AX-12* because it enables speed, position, voltage, and load control with its built-in microcontroller. It drives a gear, which in turn drives a central axle that transfers the movement to three gears, one for each switchable magnet. All gears use bearings to reduce friction and material wear.

On the center of the support there is a permanent magnet which allows the support to approach the surface before the switchable magnets are activated. Below it there is a plastic part that limits the movement of the magnetic housing. (see appendix for drawings).



Figure 5.4 Transmission mechanism, with actuator (1) and transmission mechanism (2).

The designed parts were sent to *Shapeways* to be printed on *PA 2200* plastic. ^[29]

The switchable magnets are lighter than the electromagnets; however the weight of the complex transmission mechanism they need causes the device weight (418 g) to be 3.7% bigger than the electromagnet (403 g).

5.4. Testing

The servos of the arm and the support were plugged to a *Dynamixel CM 350* main controller, and, using the *RoboPlus Task 1.1.2.2*, a code was developed to control the arm and the support, in which different commands are associated to velocity and goal position of each motor during a task. *RoboPlus Task* is a computer program which consists of instructions to control robot's actions. *RoboPlus* provides a program in *.tsk* format which is uploaded into the main controller using *RoboPlus* software.

On the experiments conducted, the switchable magnets effectively adapted and attached to the curved surface (Figure 5.5).

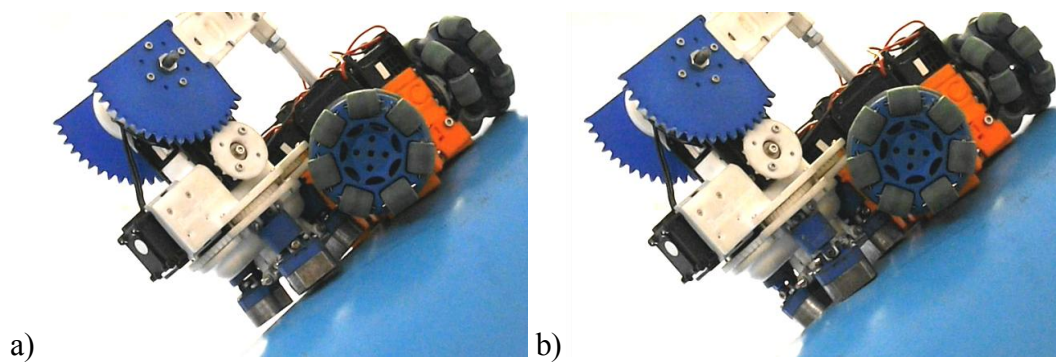


Figure 5.5 Experiment on a curved surface: a) switchable magnets off, b) on.

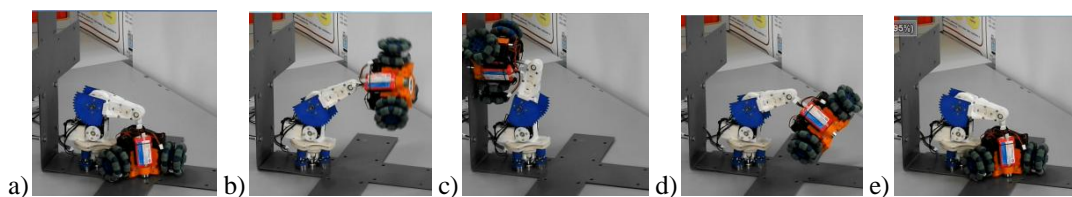


Figure 5.6 Plane transition: initial position, with the center of the *OmniClimber* 13.5 cm away from the wall, b) the robot is raised, c) the *OmniClimber* is fixed to the wall by a permanent magnet, d) It is lowered down by the arm, e) It is again on initial position.

We were able to lift the *OmniClimber* to a perpendicular wall and to take it from there. However, before we could move the *OmniClimber* from the surface, the teeth became much worn and we were not able to do more tests. This happened because while they worked fine with the older support, which was lower, the increased height of the new support caused a bigger torque that the gears could not hold for many cycles until the teeth started to wear. However, using metal gears instead of plastic ones could easily solve this problem.

6. CLIMBING ROBOT

6.1. Introduction

As a second application we tried to develop a scissor type climbing robot that relies on switchable magnets for holding.

6.2. Operation

The *SkySweeper*, developed by Nick Morozovsky, from the University of California, is designed for moving along transmission lines.^[30] It is composed by two clamps, each one driven by a motor that tightens a clamp to the cable (Figure 6.1).

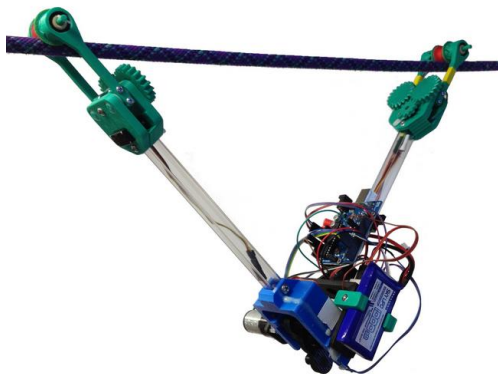


Figure 6.1 *SkySweeper*.^[30]

Inspired by this design, we developed a concept with the same configuration but instead of clamps using switchable magnets.

It has two types of magnetic adhesion on each base –dynamic and static. The dynamic adhesion is accomplished using switchable magnets, that turn on and off according to movement of the robot.

To ensure that the base is always in contact with the surface, a static adhesion is made using two permanent magnets. These are placed above the center mass to balance the bending caused by the movement of the belt.

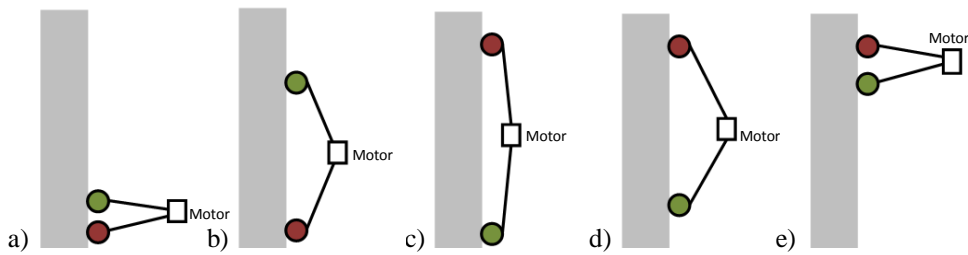


Figure 6.2 Robot behavior - the on (fixed) magnet is at red and the off (loose) at green: a) the upper magnet is off and the lower is on, and the robot is fully closed, b) the motor drives the links in order to depart from each other, c) the robot reaches its maximum extension, d) the motor turns on the opposite direction and the links begin approaching each other, e) the robot is again fully closed.

Because the switchable magnets have to be always parallel to the surface, the motor that drives the arms has also to drive two belts, each one connected to a base.

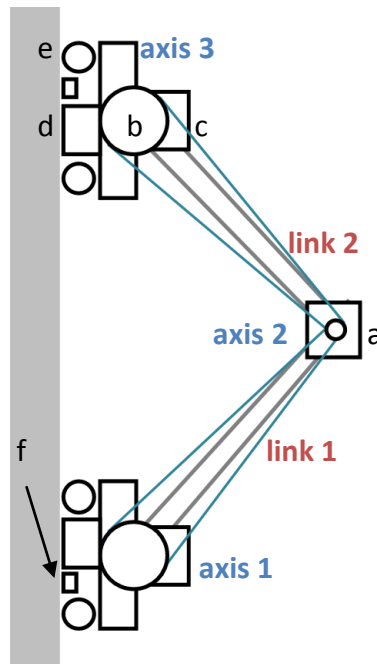


Figure 6.3 Configuration: a) motor that drives the links, b) pulley, c) motor that actuates the magnet, d) switchable magnet, e) bearing, f) permanent magnet.

To descend, the device can simply use the gravity force and as it is accelerating, be slowed down by the turning on the magnet which is on its lower end. For this process to be automatic, it requires an accelerometer to measure and control the current robot's descending acceleration. In order to have the minimum detaching torque on the tips the robot needs to be fully opened, so its center mass is as possible close to the surface.

6.3. Design

We will use a *Robotis Dynamixel AX-12* motor to activate the magnets and a *Dynamixel MX-64* to drive the links (see Appendix for data).

We made some calculations to determine the length of the links. If the arms are almost on a parallel position between each other, the torque on each axis is represented on Figure 6.4 and is given by Equations 6.1 and 6.2.

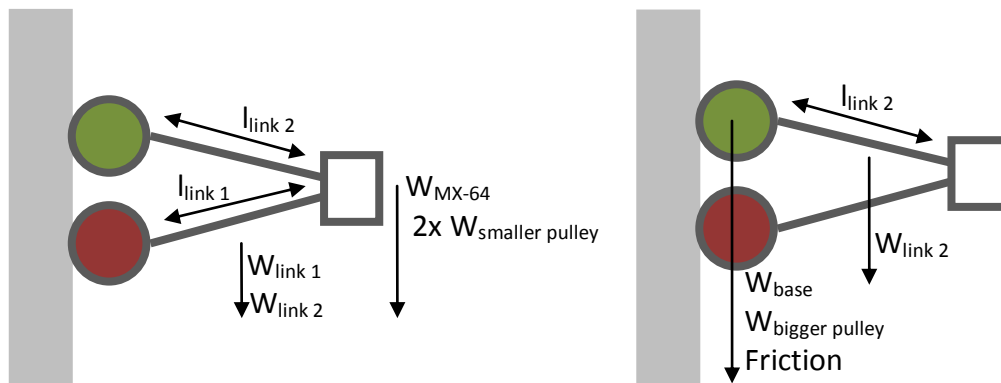


Figure 6.4 Free body diagram: a) forces from which the torque on the axis 1 depends, b) forces from which the torque on the axis 2 depends.

$$T_{axis\ 1} = l_{link\ 1} \times (W_{MX-64} + 2 \times W_{smaller\ pulley}) + \frac{l_{link\ 1}}{2} \times W_{link\ 1} + \frac{l_{link\ 2}}{2} \times W_{link\ 2} = l_{link} \times (W_{MX-64} + 2 \times W_{smaller\ pulley} + W_{link}) \quad (6.1)$$

$$T_{axis\ 2} = l_{link\ 2} \times (W_{base} + W_{bigger\ pulley} + Friction) + \frac{l_{link\ 2}}{2} \times W_{link\ 2} = l_{link} \times (W_{base} + W_{bigger\ pulley} + Friction) \times \frac{W_{link}}{2} \quad (6.2)$$

$$T_{axis\ 3} = 0 \times (W_{base} + W_{bigger\ pulley} + Friction) = 0 \quad (6.3)$$

Where:

- T is the torque;
- l is the length;
- W is the weight.

The timing belts have an efficiency of 95% to 98%. However, as we will see, the addition of a tensioner decreases considerably the overall efficiency of the system. The pulleys on the magnets have to move half the velocity of the opening of the links, so:

$$r_{bigger\ pulley} = 2r_{smaller\ pulley}$$

Because the parts move at different velocities, we need to make a formulation based on the mechanical power needed on each joint (Equation 6.4). The belt has the same velocity v in each point, so we can use it to relate the angular velocities between each others.

$$P = T \times \omega \quad (6.4)$$

$$P_{motor} = T_{motor} \times \omega_{rotor}$$

$$P_{axis\ 1} = T_{axis\ 1} \times \omega_{axis\ 1} = T_{axis\ 1} \times \frac{\omega_{rotor}}{2}$$

$$P_{axis\ 2} = T_{axis\ 2} \times \omega_{axis\ 2} = T_{axis\ 2} \times \omega_{rotor}$$

$$P_{axis\ 3} = T_{axis\ 3} \times \omega_{axis\ 3} = 0 \times \omega_{rotor} = 0$$

Where:

- P is the power;
- T is the torque;
- ω is the angular velocity.

The power required corresponds to the sum of the torque on each axis:

$$P_{motor} = P_1 + P_2 + P_3 \quad (6.5)$$

$$T_{motor} \times \omega_{rotor} = T_{axis\ 1} \times \frac{\omega_{rotor}}{2} + T_{axis\ 2} \times \omega_{rotor} + 0$$

$$T_{motor} = \frac{T_{axis\ 1}}{2} + T_{axis\ 2}$$

Replacing by Equations 6.1, 6.2 and 6.3:

$$\begin{aligned}
 T_{motor} &= l_{link} \times \left(\frac{W_{MX-64} + 2 \times W_{smaller\ pulley} + W_{link}}{2} + W_{base} + W_{bigger\ pulley} \right. \\
 &\quad \left. + Friction + \frac{W_{link}}{2} \right) \\
 &= l_{link} \\
 &\quad \times \left(\frac{W_{MX-64} + 2 \times W_{smaller\ pulley}}{2} + W_{base} + W_{bigger\ pulley} + Friction \right. \\
 &\quad \left. + W_{link} \right)
 \end{aligned}$$

We made experimental tests with the base to find its friction, and the results had an average of 6.1 N and the standard deviation of 0.28 N.

Table 6.1. Constant values

Base weight	185 g
Friction	6.1 N
Tip weight	185 g
Small pulley weight	20 g
Big pulley weight	69 g
MX-64 weight	126 g
Link weight	6 x 23 g
Link length	286 mm

Using Table 6.1 values the resulting torque is 3.08 N.m. It is far below the motor limit, however, in practical testing this proved to be impractical. The motor can reach a high torque in a short period of time, however, it needs to hold the force while the magnets are not fixed. There is also a big bending component that is one of the causes for the actuator not be able to lift the robot. Other aspect which has some influence on the overall efficiency of the mechanism is the method used for tensioning the belt. We tested ball bearings, pulleys on the middle of the belt and bars enclosing its movement but all these

solutions are associated with some loss of efficiency. Finally we stuck with the bars for simplicity of construction, but this is not a very efficient method.

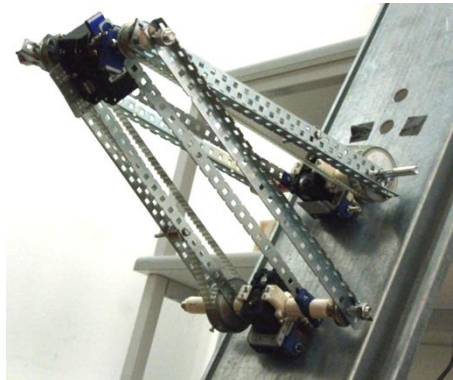


Figure 6.5 First prototype (with longer links).

Because we had some problems with the motor shutting down due to excessive load, we opted to try this device with smaller links.

Table 6.2. Updated constant values

Link weight	6 x 15 g
Link length	156 mm

With Table 6.2 values the torque is just 1.61 N.m. The device proved to be capable of climbing a ferromagnetic wall.

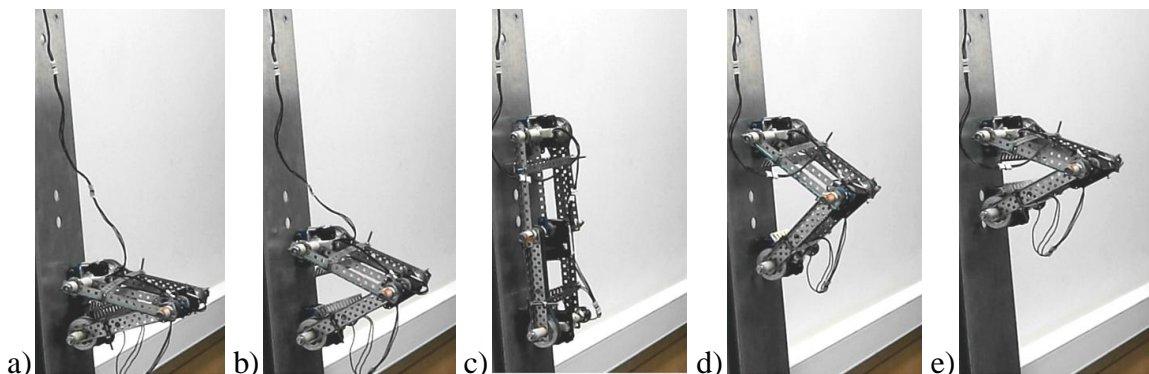


Figure 6.6 Operation (see Figure 6.2).

6.4. Features

The total weight of the robot is 754 g and its step (distance it moves during a cycle) is of 22 cm.

The *AX-12* fits on a *Robotis* kit part. Four bearings contact the surface and reduce the friction between the device and the wall. However, because the holding magnetic force varies greatly with distance, we have to put the magnetic device in a position that lets the bearings roll, but there is also still some friction between the magnetic housing and the wall. This happens because since the switchable magnet is attracted to the surface and the plastic part where it is fixed is flexible and so allows this movement, the magnetic housing is pushed against the surface of wall where the device is moving, increasing the friction.

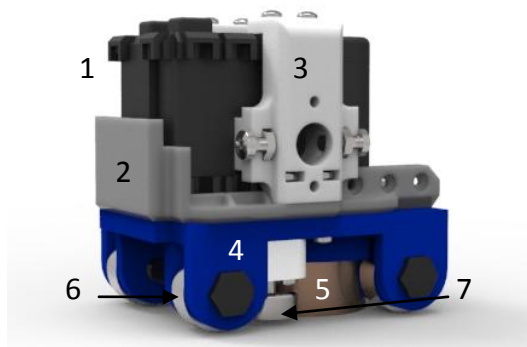


Figure 6.7 Base, with AX-12 (1), *Robotis* kit part (2), axle holder (3), magnetic support (4), switchable magnet (5), bearing (6) and permanent magnet (7).

A weight was put to counter-balance the weight of the pulleys.

Two transverse bars give rigidity to each arm and keep torsion low. The torsion is an important factor because it causes the magnet to detach to the surface and the motor also cannot work above a determined torsion value. These bars also have another function: they tight the belt to make it work under tension, otherwise the motor would have to rotate some degrees to the movement could begin being transmitted to the arm and it would not be able to secure the arm without falling some millimeters (the sufficient for the magnets to detach).

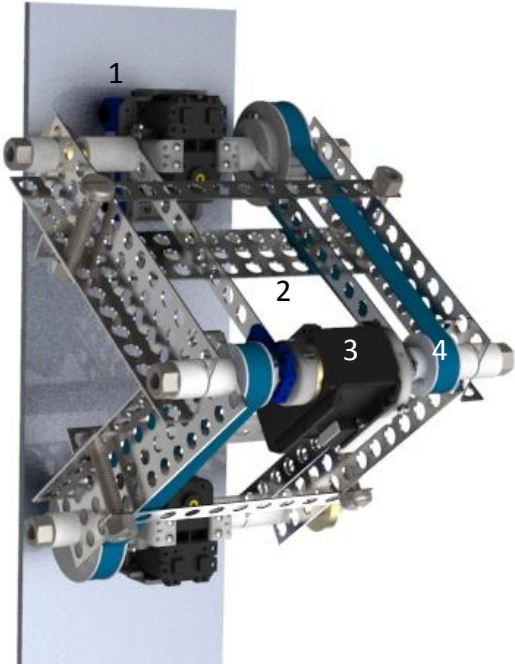


Figure 6.8 Climbing robot, with base (1), transverse bar (2), MX-64 (3) and belt (4).

7. CONCLUSION

1. We learned how different magnetic devices work and the advantages and disadvantages between each type.
2. The simulations we made on the *MagJig 95* enabled us to understand the different features of the device, allowing us to conclude that the device is already optimized in its design and technical aspects.
3. We learnt how to simulate the operation of different magnetic holders.
4. We developed a novel small scale device suitable for small robotic applications. We explored further this solution's potential by studying its force control capabilities.
5. We made two robotic applications from scratch that take advantage of switchable magnets and we were able to adjust its holding force by controlling the degree of rotation of the switchable magnets.
6. The novel *OmniClimber* support using switchable magnets was developed and successfully tested, validating our concept. However there is still a large room for improvement on its design and functioning, as we show and discuss on this work. Main issues include its weight and dimensions, which increase the torque on the robot arm and impair the robots movement. The novel climbing robot using switchable magnets was also tested successfully, although some work and further development is required to improve its reliability and performance. Nevertheless, it showed the advantages of magnetic force control with switchable magnets. With the further improvements suggested on Chapter 7.1.2, this new climbing robot can present some advantages relative to other small climbing robots such as the *OmniClimber*, by being capable of working on very small and confined places, like water pipes (Figure 7.1). Because it only needs a surface with the width of 3.8 mm to move, it can be employed in places where the others robots cannot move, especially if it is further miniaturized.

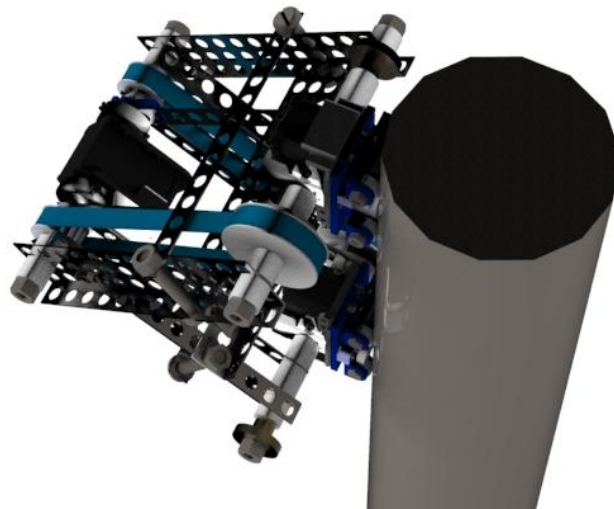


Figure 7.1 On a small section pipe.

7.1. Possible developments

7.1.1. *OmniClimber* magnetic holding device

On the electromagnet support solution, the electromagnets comprise 80 % (324 g) of the total weight, while on switchable magnet support the switchable magnets and actuator represent 43 % (181 g) of its total weight. The extra weight rests on the transmission gears and permanent magnet, so this is the area where most improvements should be made in an effort to produce a smaller and lighter solution.

One way of doing such is by developing a support with only two magnetic units and no degrees of freedom.

7.1.2. Climbing robot

The novel climbing robot using switchable magnets performed well, although some work and further development is required to improve its reliability and performance. In future work it would be interesting to have a better control of the design and technical parameters that influence the efficiency of the system, such as the belts, the magnets distance to surface and the rigidity of the whole robot structure. According to the studies made in chapter 6.4, it may have its length extended, or a less powerful motor.

A new base with springs could be developed to fit cylindrical tubes with different dimensions, a very common feature in many industrial pipes, like water pipes (Figure 7.2).

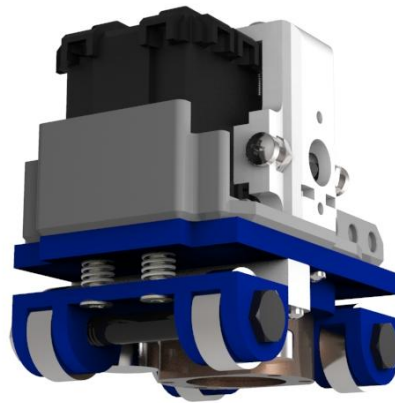


Figure 7.2 Base with springs.

7.1.3. Electropermanent magnet

Alongside the switchable magnet, another magnetic device whose potential is not being fully explored yet is the electropermanent magnet. One of the most technological ambitious projects of the last years: *Google's Project Ara*, based in the work of Ara Nerses Knaian^[17], aims to building a modular cellphone using eletropermanent magnets to attach the different modules. This means that its user would have the power to decide which physical features he would rather have his cellphone. The first model is scheduled to go the market in January 2015 for around 50 dollars.^[33]



Figure 7.3 *Project Ara* cellphone ^[32]

This magnetic device can be employed in the same applications of switchable magnets, with the advantages of not needing an actuator and/or complex transmission mechanisms. This should be the next step forward in this field of robotics.

8. LIST OF REFERENCES

1. C. Balaguer, A. Gimenez and A. Jardon, *Climbing Robots' Mobility for Inspection and Maintenance of 3D Complex Environments*, 2005.
2. Pablo Gonzalez-de-Santos – *Representative publications* [Online]. Available: <http://www.car.upm-csic.es/fsr/gds/index.html> [Accessed 3rd September 2014].
3. Manuel F. Silva and J. A. Tenreiro Machado, *A Survey of Technologies and Applications for Climbing Robots Locomotion and Adhesion*
4. *Eclipse Magnetics – Electro-holding magnets catalog* [Online]. Available: http://www.eclipse-magnetics.co.uk/files/Eclipse_Magnetics_Electro-holding_magnets_0.pdf [Accessed 3rd September 2014].
5. *RockMagnetist – StonerWohlfarthMainLoop* [Online]. Available: http://en.wikipedia.org/wiki/Magnetic_hysteresis#mediaviewer/File:StonerWohlfarthMainLoop.svg [Accessed 3rd September 2014].
6. *Dura Magnetics - What is Maximum Energy Product / BHmax and How Does It Correspond to Magnet Grade?* [Online]. Available: <http://www.duramag.com/techtalk/tech-briefs/what-is-maximum-energy-product-bhmax-and-how-does-it-correspond-to-magnet-grade> [Accessed 3rd September 2014].
7. *HKCM site* [Online]. Available: <https://www.hkcm.de/expert.php> [Accessed 3rd September 2014].
8. *Wikipedia - Diagram of Ferromagnetic Magnetic Moments* [Online]. Available: http://en.wikipedia.org/wiki/File:Diagram_of_Ferromagnetic_Magnetic_Moments.png [Accessed 3rd September 2014].
9. *Wikipedia - Diagram of Paramagnetic Magnetic Moments* [Online]. Available: http://en.wikipedia.org/wiki/File:Diagram_of_Paramagnetic_Magnetic_Moments.png [Accessed 3rd September 2014].
10. *Magnaworks Technology* [Online]. Available: <http://www.magnaworkstechnology.com/index.shtml> [Accessed 3rd September 2014].
11. *Wikimedia Commons – Electromagnetism* [Online]. Available: <http://commons.wikimedia.org/wiki/File:Electromagnetism.png> [Accessed 3rd September 2014].
12. *Chetvorno - Magnetic field of wire loop* [Online]. Available: http://en.wikipedia.org/wiki/Electromagnet#mediaviewer/File:Magnetic_field_of_wire_loop.svg [Accessed 3rd September 2014].
13. *Geek3 - VFpt Solenoid correct2* [Online]. Available: http://en.wikipedia.org/wiki/Electromagnet#mediaviewer/File:VFpt_Solenoid_correct2.svg [Accessed 3rd September 2014].
14. *Wikipedia – Electromagnet* [Online]. Available: <http://en.wikipedia.org/wiki/Electromagnet> [Accessed 3rd September 2014].
15. Yong Chen, Changming Wang, and Jiandong Bao, *Design optimization of a novel magnetic switchable device based on Halbach array*, 2013.

16. Philibert Maurice Brailon, *Magnetic plate comprising permanent magnets and electropermanent magnet*, US 4075589 A, 1978.
17. Ara Nerses Knaian, *Electropermanent Magnetic Connectors and Actuators: Devices and Their Application in Programmable Matter*, Massachusetts Institute of Technology, 2010.
18. Frederic Rochat, Patrick Schoeneich, Michael Bonani, Stephane Magnenat, Francesco Mondada, Hannes Bleuler and Christoph H. Urzeler, *Design of Magnetic Switchable Device (MSD) and applications, in climbing robot*, 2010.
19. Bey Ahmet K, *Variable magnet*, US 3223898 A, 1965.
20. Arlo F. Israelson, *Turn-off permanent magnet*, US 3452310 A, 1969
21. Perry J Underwood, Franz Kocijan, *Switchable permanent magnetic device*, US 7012495 B2, 2006.
22. Hagen Schempf, Brian Chemel, Nathan Everett, *Neptune: Above-Ground Storage Tank Inspection Robot System*, Robotics Institute, Carnegie Mellon University, 1995.
23. Kyle Gilpin, Keith Kotay, Daniela Rus, and Iuliu Vasilescu, *Miche: Modular Shape Formation by Self-Disassembly*.
24. *Magsitch - MagJig 95* [Online]. Available: <http://magswitch.com.au/product/magswitch-magjig-95>[Accessed 3rd September 2014].
25. *Comsol Multiphysics* site [Online]. Available: <http://www.comsol.com/comsol-multiphysics> [Accessed 3rd September 2014].
26. *Asom - AISI 1018 - Mild/Low Carbon Steel* [Online]. Available: <http://www.azom.com/article.aspx?ArticleID=6115>
27. Carlos Viegas, Mahmoud Tavakoli, *A Single DOF arm for transition of climbing robots between perpendicular planes*, 2014.
28. *Trossen Robotis - Dynamixel AX-12A Robot Actuator* [Online]. Available: <http://www.trossenrobotics.com/dynamixel-ax-12-robot-actuator.aspx> [Accessed 3rd September 2014].
29. *Shapeways - PA 2000 - Material data sheet* [Online]. Available: https://www.shapeways.com/rrstatic/material_docs/mds-strongflex.pdf [Accessed 3rd September 2014].
30. *Maker Media 2013 - SkySweeper* [Online]. Available: <http://review.wizehive.com/voting/view/makermedia2013/15849/1387186/0> [Accessed 3rd September 2014].
31. *Trossen Robotis - Dynamixel MX-64T Robot Actuator* [Online]. Available: <http://www.trossenrobotics.com/p/mx-64t-dynamixel-robot-actuator.aspx> [Accessed 3rd September 2014].
32. *Motorola - Project_Ara_scattered_parts.png* [Online]. Available: http://en.wikipedia.org/wiki/File:Project_Ara_scattered_parts.png [Accessed 3rd September 2014].
33. *CNET - Google targeting Project Ara modular phone for January 2015*[Online]. Available: <http://www.cnet.com/news/google-targeting-project-ara-phone-for-january-2015/>[Accessed 3rd September 2014].

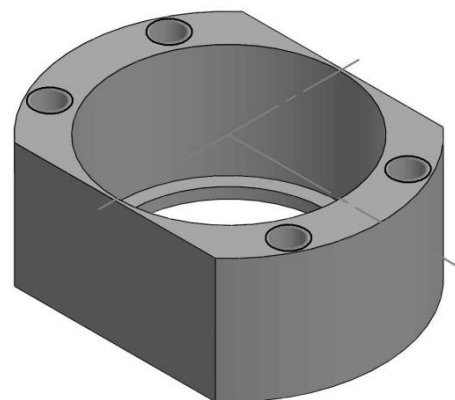
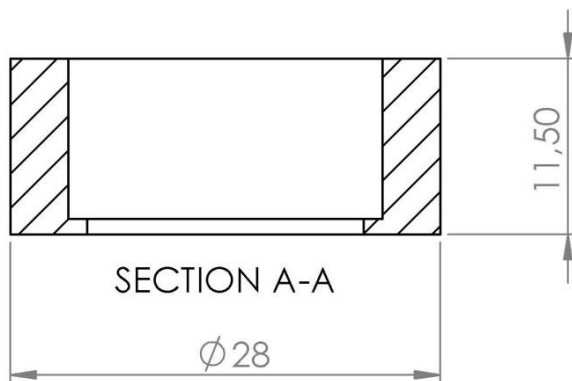
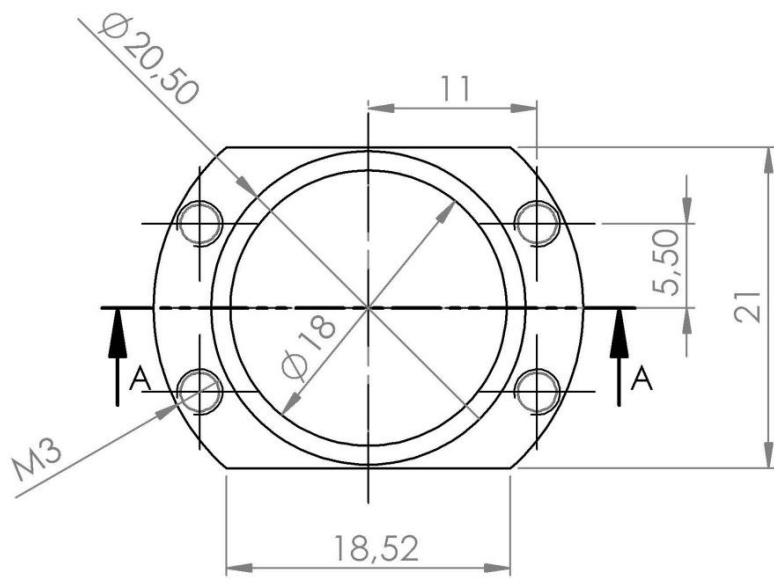
9. APPENDIX

AX-12 data ^[28]

Operating voltage	12 V
Stall torque	15.3 kg·cm
No-load speed	59 RPM
Weight	55g
Size	32 x 50 x 40 mm
Resolution	0.29°
Reduction ratio	1/254
Operating angle	300° or continuous turn
Operating voltage	9-12V (recommended voltage - 11.1V)
Max current	900 mA
Standby current	50 mA
Operating temperature	-5°C ~ 85°C

MX-64 data ^[28]

Operating voltage	14.8 V	12 V
Stall torque	7.3 N.m	6.0 N.m
No-load speed	78 RPM	63 RPM
Weight	126g	
Size	40.2 x 61.1 x 41.0 mm	
Resolution	0.088°	
Reduction ratio	1/200	
Operating angle	360° or continuous turn	
Max current	4.1A @ 12V	
Standby current	100 mA	
Operating temperature	-5°C ~ 80°C	



UNLESS OTHERWISE SPECIFIED:
 DIMENSIONS ARE IN MILLIMETERS
 SURFACE FINISH:
 TOLERANCES:
 LINEAR:
 ANGULAR:

FINISH:

DEBUR AND
 BREAK SHARP
 EDGES

DO NOT SCALE DRAWING

REVISION

NAME	SIGNATURE	DATE			
DRAWN					
CHK'D					
APPV'D					
MFG					
Q.A					
			MATERIAL:		
			WEIGHT:		

TITLE:

DWG NO.

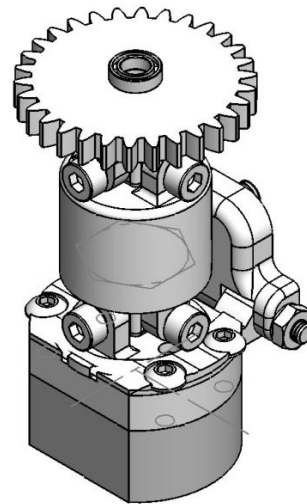
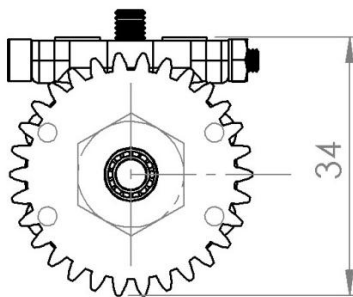
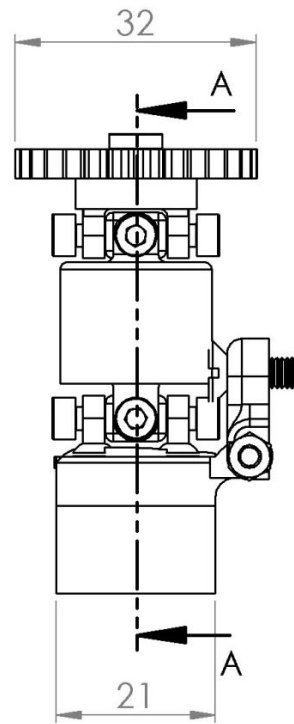
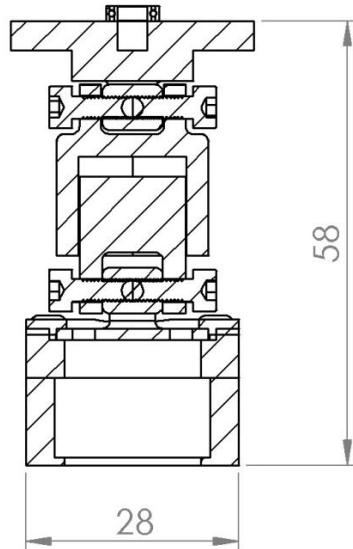
Novel housing

A4

SCALE:2:1

SHEET 1 OF 1

SECTION A-A



UNLESS OTHERWISE SPECIFIED:
DIMENSIONS ARE IN MILLIMETERS
SURFACE FINISH:
TOLERANCES:
LINEAR:
ANGULAR:

FINISH:

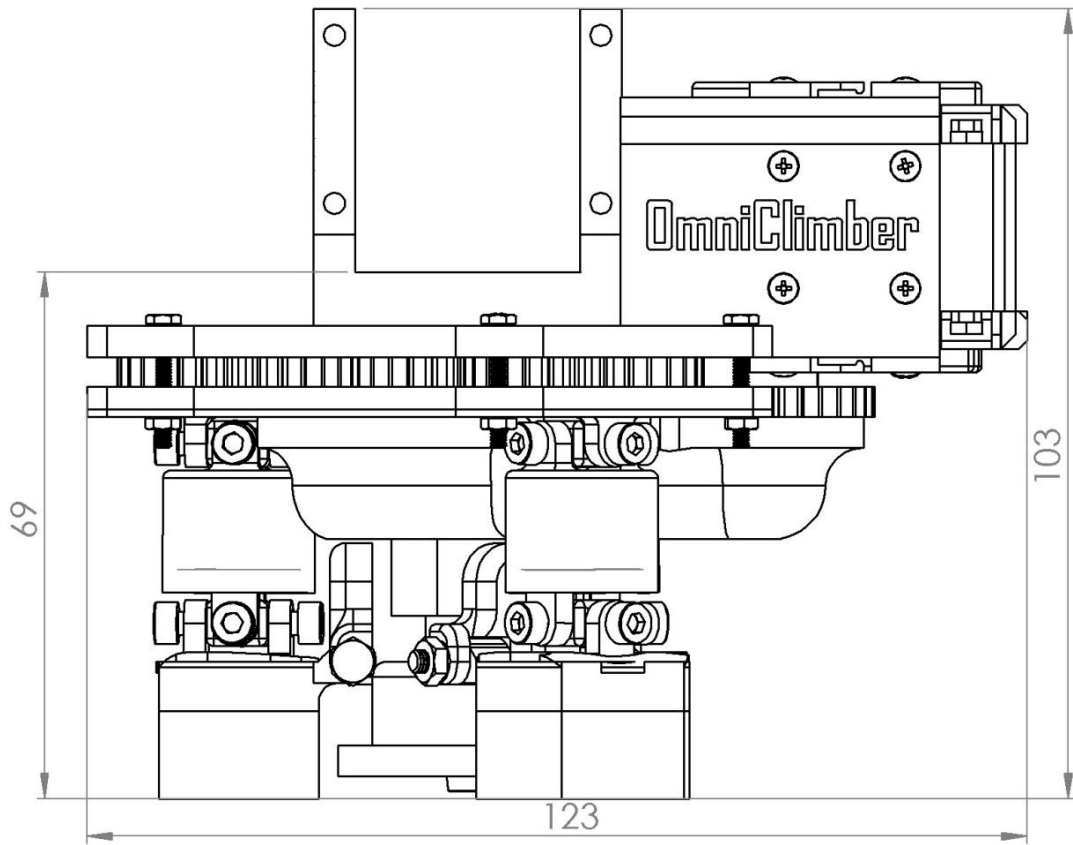
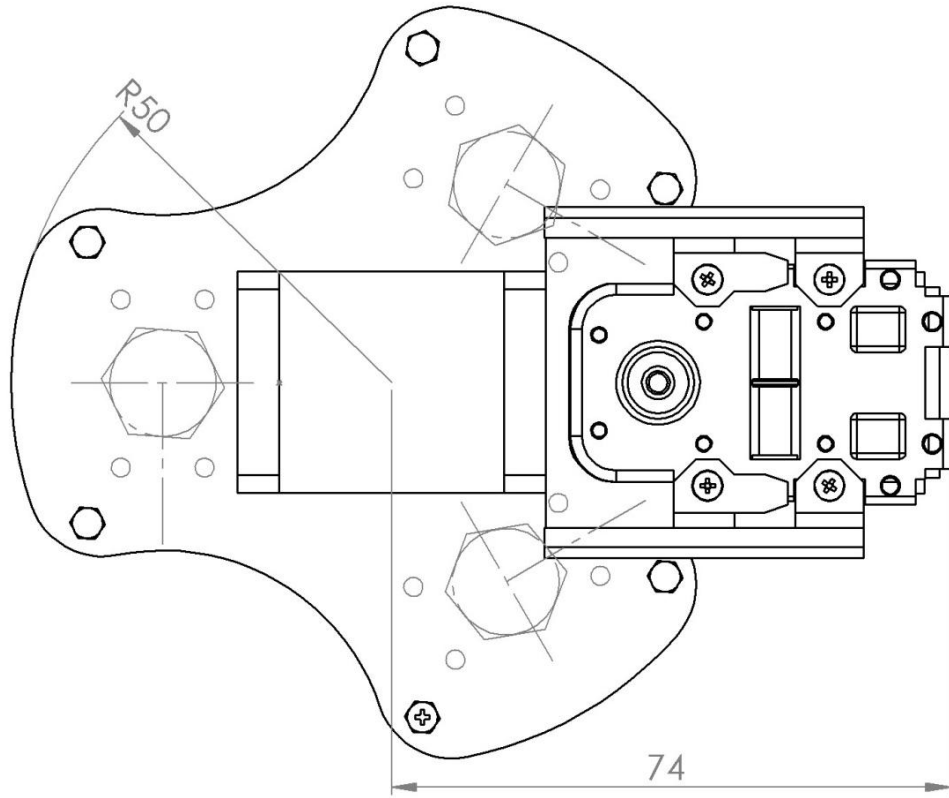
DEBUR AND
BREAK SHARP
EDGES

DO NOT SCALE DRAWING

REVISION

	NAME	SIGNATURE	DATE		
DRAWN					
CHK'D					
APP'VD					
MFG					
Q.A					
				MATERIAL:	
				WEIGHT:	

TITLE:		
DWG NO.	Transmission axle	A4
SCALE:1:1	SHEET 1 OF 1	



UNLESS OTHERWISE SPECIFIED:
 DIMENSIONS ARE IN MILLIMETERS
 SURFACE FINISH:
 TOLERANCES:
 LINEAR:
 ANGULAR:

FINISH:

DEBUR AND
 BREAK SHARP
 EDGES

DO NOT SCALE DRAWING

REVISION

NAME	SIGNATURE	DATE			
DRAWN					
CHK'D					
APPV'D					
MFG					
Q.A					
				MATERIAL:	
				WEIGHT:	

TITLE:

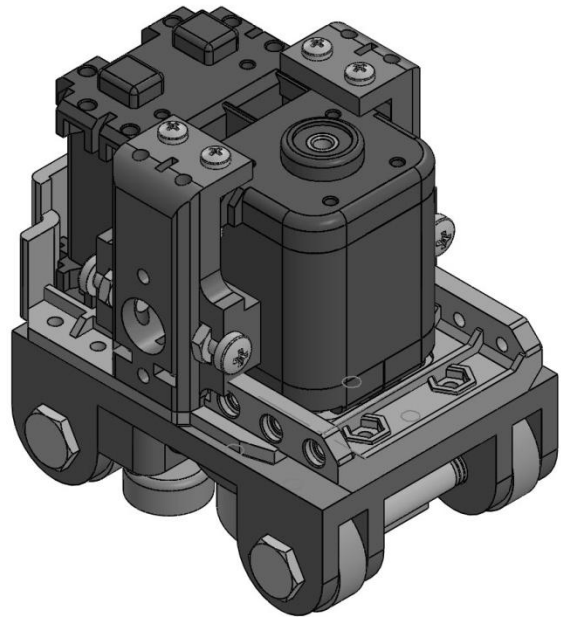
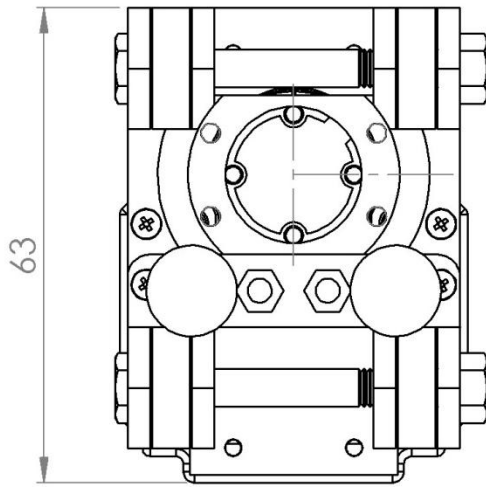
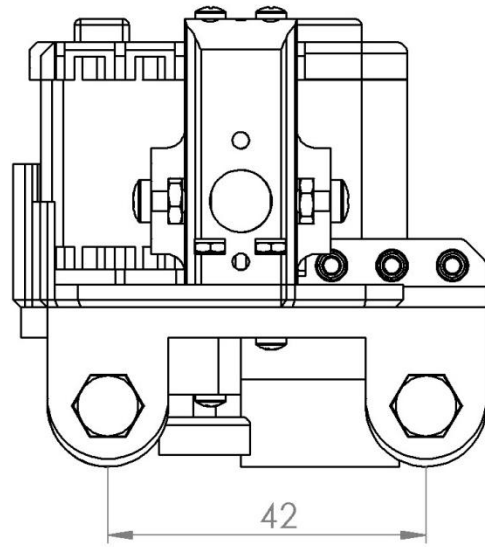
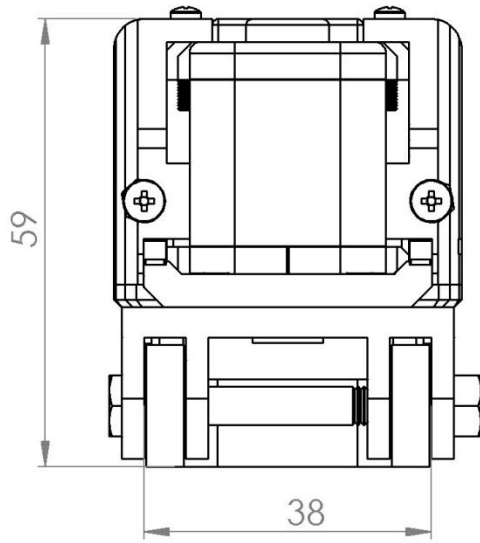
DWG NO:

OmniClimber support

A4

SCALE:1:1

SHEET 1 OF 1



UNLESS OTHERWISE SPECIFIED:
DIMENSIONS ARE IN MILLIMETERS
SURFACE FINISH:
TOLERANCES:
LINEAR:
ANGULAR:

FINISH:

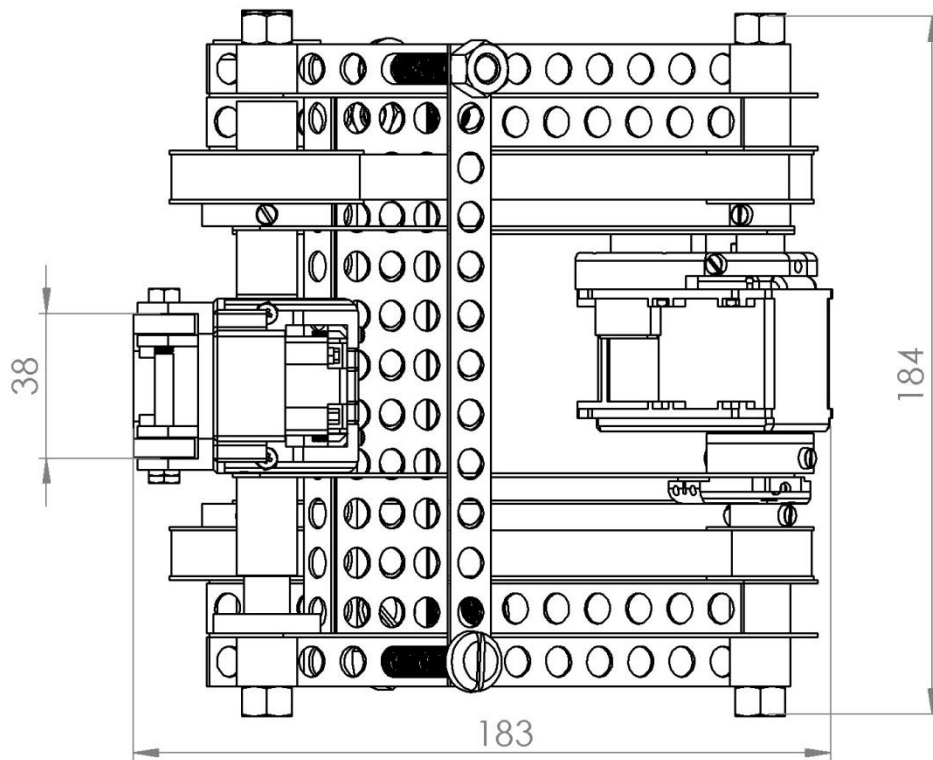
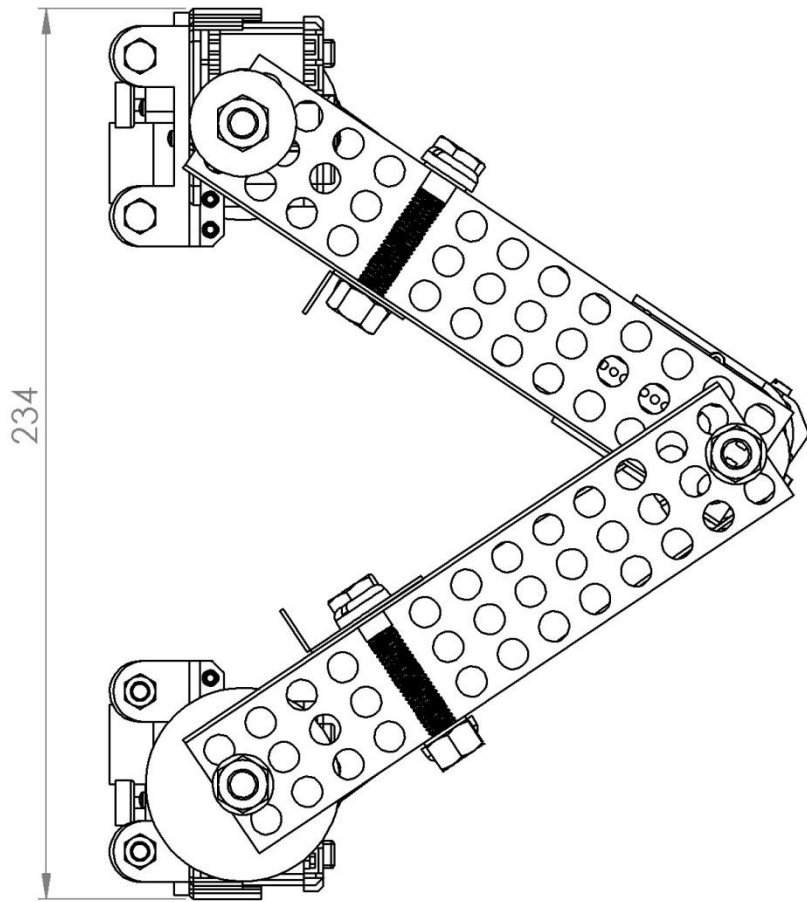
DEBUR AND
BREAK SHARP
EDGES

DO NOT SCALE DRAWING

REVISION

	NAME	SIGNATURE	DATE		
DRAWN					
CHK'D					
APPV'D					
MFG					
Q.A				MATERIAL:	
				WEIGHT:	

TITLE:	
DWG NO.	Base
SCALE:1:1	SHEET 1 OF 1
	A4



UNLESS OTHERWISE SPECIFIED:
DIMENSIONS ARE IN MILLIMETERS
SURFACE FINISH:
TOLERANCES:
LINEAR:
ANGULAR:

FINISH:

DEBUR AND
BREAK SHARP
EDGES

DO NOT SCALE DRAWING

REVISION

NAME	SIGNATURE	DATE		
DRAWN				
CHK'D				
APPV'D				
MFG				
Q.A				
			MATERIAL:	
			WEIGHT:	

TITLE:	
DWG NO.	Climbing robot
SCALE:1:2	A4
SHEET 1 OF 1	